A STUDY OF THE INORGANIC CARBON CYCLING ON THE SCOTIAN SHELF

by

Wanying Ji

Submitted in partial fulfillment of the requirements
for the degree of Master of Science

at

Dalhousie University
Halifax, Nova Scotia
September 2019

TABLE OF CONTENTS

LIST OF TABLES

LIST OF FIGURES

ABSTRACT

The stable carbon isotopic composition ($\delta^{13}C_{DIC}$) of dissolved inorganic carbon (DIC) can be used as an effective indicator of biological processes in carbon cycling, however, so far, few, if any, studies have been conducted on Scotian Shelf (NW Atlantic) waters focusing on $\delta^{13}C_{DIC}$. In this study, the spatial and temporal distribution of DIC and $\delta^{13}C_{DIC}$ in Scotian Shelf waters and their governing processes are investigated. Samples were collected on the Scotian Shelf during April and October cruises in 2014 on the Canadian Coast Guard Ship Hudson. Throughout the research period, a combination of biological processes and the freshwater input resulted in the changes of DIC concentration and $\delta^{13}C_{DIC}$ value in the Scotian Shelf waters. The monthly NCP on the surface water of the study region ranges from -0.76 to 0.57 molC m^{-2} $month^{-1}$, and reveals both autotrophic and heterotrophic regions in the mixed layer of the Scotian Shelf.

LIST OF ABBREVIATIONS AND SYMBOLS USED

Roman Symbol	Description	Units
Chl-*a*	Chlorophyll-*a* concentration	$\mu g\ m^{-3}$
CO_2	Carbon Dioxide	no units
Cumulative NCP	Cumulative NCP over six months	$molC\ m^{-2}$
DIC	Dissolved Inorganic Carbon	$\mu mol\ kg^{-1}$
DIC_{avg}	Average DIC concentration	$\mu mol\ kg^{-1}$
DIC_{bio}	Biological component of DIC	$\mu mol\ kg^{-1}$
DIC_{pCO2}	DIC concentration at atmospheric equilibrium	$\mu mol\ kg^{-1}$
$\delta^{13}C_{DIC}$	Stable isotopic composition of DIC	‰VPDB
f	Biological fractionation factor	‰
k	Slope of the relationship between $\delta^{13}C_{DIC}$ and the dissolved phosphate concentration	‰VPDB per $\mu molC\ kg^{-1}$
NCP	Net community production	$molC\ m^{-2}\ month^{-1}$
NPP	Net primary production	$molC\ m^{-2}\ month^{-1}$
R	Heterotrophic respiration	$molC\ m^{-2}\ month^{-1}$
TA	Total Alkalinity	$\mu mol\ kg^{-1}$
VPDB	Vienna Pee Dee Belemnite	no units

ACKNOWLEDGEMENTS

I would first like to thank my supervisor Helmuth Thomas, who has given me opportunities to pursue my graduate study; who has provided me guidance and support throughout the way; who has always trusted me being able to accomplish any tasks or challenges; who has never refused to answer any question I asked; who has given me enormous confident in myself without himself knowing. I would also like to thank my committee members Christopher Algar and Markus Kienast, who have given me critical advice and insightful suggestions to help me build up my thesis. I also would like to thank Jonathan Lemay and Jacoba Mol for collecting data and analyzing samples. Finally, I want to express my very profound gratitude to my family and friends (Mohammad Abdulrahman, Bin Wang, Shangfei Lin, Jenna Hare, Lin Cheng, Lida Abdulrahman, Katie Gordon, Qiang Shi and many others) for providing me with unfailing support and continuous encouragement throughout my study years. This accomplishment would not have been possible without them. Thank you.

CHAPTER 1. INTRODUCTION

1.1 Motivation

Carbon dioxide (CO_2) emissions from fossil fuel combustion (Archer, Kheshgi, & Maier-Reimer, 1997) and land-use change have been increasing over the last 150 years (Parry et al., 2007; IPCC, 2007; Montenegro, 2007). This anthropogenic carbon dioxide contributed to the total concentration of CO_2 in the atmosphere, and the average global atmospheric CO_2 concentration has reached 412 ppm in 2019 (NASA, 2019). The increased atmospheric CO_2 concentration due to anthropogenic activities has affected the global climate as well as the global ocean (Parizek & Alley, 2004; Bindoff et al., 2007; Solomon et al., 2009). About 27% of the anthropogenic CO_2 emissions from the year 2004 to the year 2013 has been absorbed by the ocean (Le Quéré et al., 2014). Therefore, the ocean plays a fundamental role in the air-sea carbon cycling system as they constitute significant CO_2 sinks. The majority of the carbon in the air-sea system is stored in the ocean as dissolved inorganic carbon (DIC) (Houghton, 2003). The invasion of anthropogenic CO_2 into the ocean has led to a reduction of ocean pH and carbonate ion concentrations, which is referred to as ocean acidification (Orr et al., 2005; Montenegro, 2007; Doney et al., 2009; Shadwick, 2010).

Coastal oceans make up approximately 7% of the surface area of the global ocean (Gattuso, Frankignoulle & Wollast, 1998). However, they play an essential role in the biogeochemical cycling of carbon. As a link between terrestrial and oceanic systems, coastal areas are highly dynamic with large variations in hydrographic properties. They also receive a substantial amount of nutrients and carbon from rivers and upwelling waters,

which often results in high biological activities in the surface water (about 10-30% of the oceanic primary productivity) (Gattuso, Frankignoulle & Wollast, 1998; Shadwick & Thomas, 2014; Clargo et al., 2015). Although coastal oceans are important to ocean carbon cycling, their CO_2 system has remained relatively understudied in comparison to the open ocean (Smith & Hollibaugh, 1993; Wollast, 1998; Gattuso, Frankignoulle & Wollast, 1998; Shadwick, 2010; Burt et al., 2016). In 2015, Gledhill et al. suggested that some coastal regions, such as the Scotian Shelf, are more vulnerable to coastal ocean acidification in response to changes in the timing and volume of freshwater inputs. In order to assess the current status of carbonic species in Scotian Shelf waters and characterize the role that this continental shelf plays in the carbon cycling system of coastal oceans, a proper baseline for the spatial and seasonal distributions of DIC and its the stable carbon isotopic composition ($\delta^{13}C_{DIC}$) will be established.

In this research, the seasonal and spatial distribution of $\delta^{13}C_{DIC}$ and DIC in Scotian Shelf waters, as well as their governing processes, will be examined. The results of this study will provide more detailed insight into the inorganic carbon cycling on the Scotian Shelf and present a baseline of $\delta^{13}C_{DIC}$ data for future studies.

1.2 Oceanographic Setting

The Scotian Shelf is an open continental shelf that is approximately 200 km wide and 700 km long, adjacent to the province of Nova Scotia along the eastern Coast of Canada (Fournier et al., 1977; Loder et al., 1997) (Fig. 1). It is bordered by the Laurentian Channel to the northeast, the Northeast Channel and the Gulf of Maine to the southwest, and the total area of the shelf covers approximately 120,000 km^2. The shelf is located at the

boundary between the subpolar and subtropical gyres, downstream of the Gulf of St. Lawrence (GSL), which leads to large spatial and temporal variations in its hydrographic properties (Petrie & Drinkwater, 1993; Loder et al., 1997) (Fig. 1).

In warm seasons (summer and fall), there are three end-members on the Scotian Shelf: the St. Lawrence Estuary Water (SLEW), the Labrador Shelf water (LShW), and the Warm Slope water (WSW). The St. Lawrence River discharges river water into the SLEW and provides the majority of freshwater into the Scotian Shelf (Shadwick, 2010; Rutherford & Fennel, 2018). Since the salinity of surface water in the Laurentian Channel in the GSL ranges between 27 and 32 (Mucci et al., 2011), water with a salinity lower than 32 is considered as freshwater in this study. The LShW flows into the Gulf of St. Lawrence along the southwest coast of Newfoundland through the Cabot Strait and also via the inner branch of the Labrador Current along the northwest coast of Newfoundland through the Strait of Belle Isle. The SLEW mixes with the LShW and exits the Gulf of St. Lawrence via the northwest side of Cabot Strait, creating an inner shelf flow on the Scotian Shelf, known as the Nova Scotia Current (NSC) (Chapman & Beardsley, 1989; Petrie & Drinkwater, 1993). Additionally, this outflow creates a shelf break current, which joins an extension of the Labrador Current and flows along the shelf break towards the southwest (Chapman & Beardsley, 1989; Petrie & Drinkwater, 1993; Loder et al., 1997; Hannah et al., 2001; Shadwick et al., 2010) (Fig. 1). The water exiting the Cabot Strait feeds the NSC and generates a salinity minimum on the Scotian Shelf in late summer (Loder et al., 1997; Gledhill et al., 2015, Shadwick, 2010). Reciprocally, the Scotian Shelf receives minimal water from the St. Lawrence Estuary Water in winter and early spring due to the formation of sea ice in the Gulf of St. Lawrence. As a result, during these seasons, the NSC is strongly dominated by the LShW (see also Shadwick & Thomas, 2011, their Fig. 3.5). Thus, in

winter and early spring, there are only two end members influencing the Scotian Shelf water: the LShW and the WSW. The WSW is the Labrador Slope Water modified by the warm saline water from the north-easterly flowing Gulf Stream (Gatien, 1976; Fournier et al., 1977). It is characterized by its high nutrient concentrations, which are provided from the deep North Atlantic Central Water (NACW) beneath (Gatien, 1976; Townsend et al., 2015). We will verify these general hydrographic features later (sect. 3.1) against our observations.

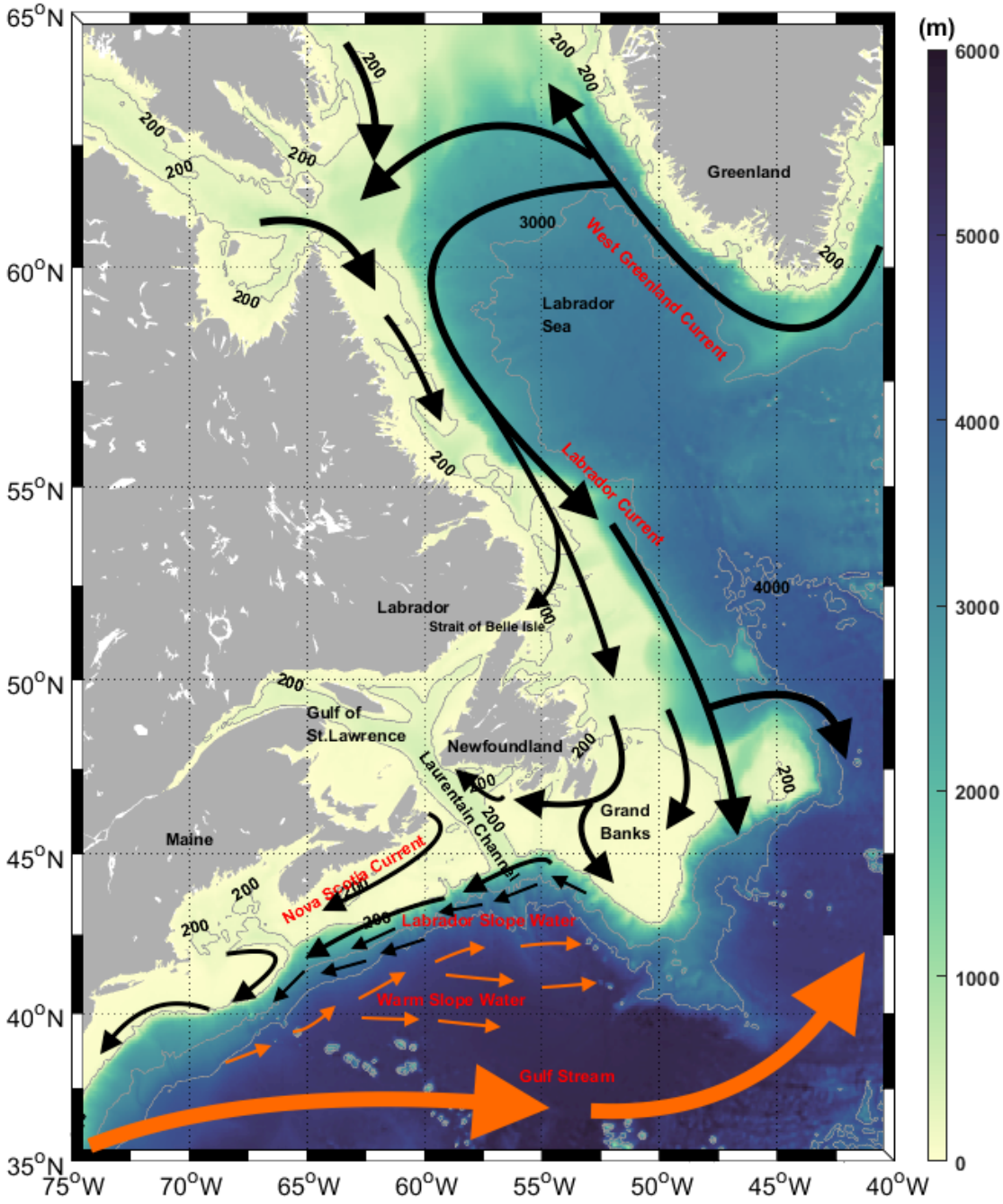

Fig. 1. Scotian Shelf bathymetry. The black arrows indicate long-term mean surface circulation and the orange arrows indicate the flowing direction of Gulf Stream and Warm Slope Water. The color bar indicates the depth of the water. The contour lines from nearshore to offshore are 200m, 2000m, 3000m, and 4000m, respectively.

The Scotian Shelf is characterized as a rich ecosystem that supports diverse marine life communities and habitats (Atlantic Coastal Zone Information Steering Committee,

2016). It provides food and shelter for a variety of species ranging from microscopic plankton to whales (Fisheries and Oceans Canada, 2014b, p. 14). It also supports essential fisheries, as well as aquaculture, and is impacted by oil and gas exploration (Shadwick, 2010; Fisheries and Oceans Canada, 2014a). Thus, the Scotian Shelf is important to local communities, both economically and environmentally. A better understanding of the Scotian Shelf will be beneficial to local communities who aim for a sustainable exploitation of living marine resources of the region; it will also contribute to quantifying the role of coastal oceans in the North Atlantic uptake of atmospheric CO_2.

1.3 Carbonate Chemistry

Atmospheric CO_2 enters the ocean and reacts with water to form an unstable product: carbonic acid (Equation 1.1). This acid dissociates by equation 1.2 and 1.3 (Dickson, 2007).

$$CO_{2(aq)} + H_2O_{(l)} \rightleftharpoons H_2CO_{3(aq)} \quad (1.1)$$

$$H_2CO_{3(aq)} \rightleftharpoons H^+_{(aq)} + HCO^-_{3(aq)} \quad (1.2)$$

$$HCO^-_{3(aq)} \rightleftharpoons H^+_{(aq)} + CO^{2-}_{3(aq)} \quad (1.3)$$

H_2CO_3 is found only in small quantities compared to the other carbonate species and it is operationally indistinguishable from $CO^*_{2(aq)}$, where $CO^*_{2(aq)}$ is the sum of $CO_{2(g)}$ and H_2CO_3. Hence, equation 1.4 is often used to substitute equation 1.1 and 1.2.

$$CO^*_{2(aq)} + H_2O_{(l)} \rightleftharpoons HCO^-_{3(aq)} + H^+_{(aq)} \quad (1.4)$$

The reactions are also important in regulating the pH in seawater and gas exchanges between air-sea as well as the biosphere.

$[HCO_3^-]$ and $[CO_3^{2-}]$ are very difficult to measure individually; thus DIC is used (Equation 1.5), which can be measured by acidifying the solution and measuring the resulting CO_2.

$$DIC = \left[CO^*_{2(aq)}\right] + [HCO_3^-] + [CO_3^{2-}] \quad (1.5)$$

Several processes can affect DIC concentrations in oceans, for instance, photosynthesis and remineralization of organic matter. Phytoplankton assimilates DIC from seawater into organic carbon, which leads to a decrease in DIC, while remineralization causes the opposite result. Other processes, for instance, CO_2 invasion and degassing through air-sea exchange, and calcium carbonate ($CaCO_3$) dissolution and precipitation can also affect DIC concentrations in the ocean (e.g., Zeebe & Wolf-Gladrow, 2001; Winde et al., 2014a).

Total alkalinity (TA), another measurable quantity, is not affected by changes in temperature or pressure, making it an effective variable to explain CO_2 cycling. It can be defined as a charge balance of major ions in seawater (equation 1.6 & 1.7),

$$TA = \Sigma(charges\ of\ all\ cations) - \Sigma(charges\ of\ anions\ of\ strong\ acids) \quad (1.6)$$

with strong acids defined by pKa < 4.5 at 25°C.

$$TA = [Na^+] + 2[Mg^{2+}] + 2[Ca^{2+}] + [K^+] - [Cl^-] - 2[SO_4^{2-}] - [NO_3^-] \quad (1.7)$$

Total alkalinity can also be defined with respect to the buffer capacity of seawater (equation 1.8). It is calculated as the excess of bases (proton acceptors) of weak acids over strong acids (proton donors), where weak acids are defined as pKa > 4.5 at 25°C.

$$TA = [HCO_3^-] + 2[CO_3^{2-}] + [B(OH)_4^-] + [OH^-] + [SiO(OH)_3^-] + [HPO_4^{2-}] + 2[PO_4^{3-}] + [HS^-] + [NH_3] - [H_3O^+] - [HSO_4^-] - [HF] - [H_3PO_4] \quad (1.8)$$

The equation can be approximated as,

$$TA \approx [HCO_3^-] + 2[CO_3^{2-}] + [B(OH)_4^-] + [OH^-] - [H_3O^+] \quad (1.9)$$

where more minor components are neglected.

Processes such as $CaCO_3$ precipitation and dissolution as well as assimilation and remineralization of nitrogen can affect TA in the ocean: the dissolution of $CaCO_3$ increases both DIC and TA in the ratio of 1:2 (e.g., Zeebe & Wolf-Gladrow, 2001); the consumption of nitrate (NO_3^-) during assimilation leads to an increase in TA. (e.g., Brewer & Goldman, 1976).

1.4 Isotopic Composition of Dissolved Inorganic Carbon ($\delta^{13}C_{DIC}$)

In nature, there are three forms of carbon isotopes. The most abundant form is carbon-12 (^{12}C), containing six protons and six neutrons, with a relative abundance of 98.9%. Only 1.1% of carbon on Earth is of Carbon-13 (^{13}C) isotopic form, which contains seven neutrons. Both ^{12}C and ^{13}C are stable while carbon-14 (^{14}C), which contains eight neutrons, is radioactive and decays into a stable product ($^{14}_{7}N$); thus, its relative abundance is less than 0.0001% (NOAA, 2005).

$\delta^{13}C_{DIC}$ denotes the stable carbon isotopic composition of dissolved inorganic carbon. It is calculated by relating it to a VPDB (Vienna Pee Dee Belemnite) standard (see equation 2.1). The VPDB standard for ^{13}C is established based on the sample of a Cretaceous marine fossil (*Beleminatella americana*) found in South Carolina (Craig, 1953, 1957). $\delta^{13}C_{DIC}$ is controlled by several factors including biological processes (production and respiration of organic matter) (Wong & Sackett, 1978; Lynch-Stieglitz et al., 1995 ; Schmittner et al., 2013), thermodynamic fractionation (Mook, Bommerson & Staverman,1974), air-sea exchange (Broecker & Peng, 1974; Keeling, 1979 ; Mackensen,

2013), the addition of freshwater, and calcium carbonate ($CaCO_3$) dissolution and formation (Winde et al., 2014a; Eide et al., 2017b).

In the open ocean, the $\delta^{13}C_{DIC}$ signal is governed by a balance of biological and thermodynamic processes (Gruber et al., 1999; Schmittner et al., 2013), while air-sea exchange can also influence the $\delta^{13}C_{DIC}$ signal (Tans, 1980; Lynch-Stieglitz et al., 1995). As a vast amount of isotopically light carbon has been added into the atmosphere from fossil fuel burning over centuries, the proportion of ^{12}C, ^{13}C, and ^{14}C in both the atmosphere and ocean have shifted (Keeling, 1979; Quay et al., 1992). This is known as the "Suess effect," which has altered the $\delta^{13}C_{DIC}$ signal from the 1970s to the 1990s in the surface waters of the global ocean by -0.160±0.02‰ per decade (Quay et al., 2003). As a result, $\delta^{13}C_{DIC}$ signals can be used to estimate the accumulation rate of anthropogenic carbon in surface waters and estimate the Suess effect in the global ocean (Quay et al., 2007; Olsen & Ninnemann, 2010; Eide et al., 2017 a,b)

In coastal ocean systems, the spatial and temporal variabilities of $\delta^{13}C_{DIC}$ are more pronounced compared to the open ocean (Gruber et al. 1999; Burt et al., 2016), and are predominantly governed by biological processes and freshwater input. Marine primary producers preferentially take up the light carbon (^{12}C) when assimilating the dissolved inorganic carbon from seawater into organic carbon during photosynthesis, since ^{13}C forms stronger chemical bonds than ^{12}C and takes longer time to break (O'Leary, 1988). The assimilation process leaves the heavier ^{13}C behind, which increases the $\delta^{13}C_{DIC}$ values in the surface water (O'Leary, 1981). In contrast, respiration of organic matters releases the isotopically light carbon back into the water column, which increases the DIC concentrations while decreasing the $\delta^{13}C_{DIC}$ values (O'Leary, 1981). This kinetic

fractionation plays an important role in governing the $\delta^{13}C_{DIC}$ variations in coastal regions. Since rivers are often depleted in $\delta^{13}C_{DIC}$ (ranges from zero to as low as -25 ‰VPDB) due to the dissolution of biogenic carbon ($\delta^{13}C_{DIC} \cong$ -25 ‰VPDB) in soils (Spiker, 1980), the freshwater sources tend to confound the $\delta^{13}C_{DIC}$ signal in coastal regions (Burt et al., 2016). As a result, the governing processes of $\delta^{13}C_{DIC}$ distributions and their mechanisms are less established in coastal oceans, compared to the open oceans (Smith & Hollibaugh, 1993; Ostrom et al., 1997; Wollast, 1998; Gattuso, Frankignoulle & Wollast, 1998). Other factors, such as calcification, is not considered as a significant contributor for changing $\delta^{13}C_{DIC}$ compared to factors such as biological processes and river inputs. Eide et al. (2017) suggest that the thermodynamic process factor in altering $\delta^{13}C_{DIC}$ signal can also be neglected. Cold water tends to have higher $\delta^{13}C_{DIC}$ than warm water at air-sea isotopic equilibrium (Mook, Bommerson & Staverman, 1974); however, this equilibrium rarely exists in coastal waters, and the overall influence of thermodynamic fraction is relented (Lynch-Stieglitz et al., 1995; Schmittner et al., 2013).

$\delta^{13}C_{DIC}$ is of particular value for identifying sources, sinks, and transformations of carbon in water columns (Sackett and Moore, 1966; Deines et al., 1974; Böttcher, 1999; Fry, 2002; Dorsett et al., 2011; Mackensen, 2013; Burt et al., 2016), as well as identifying benthic-pelagic coupling (Ostrom et al., 1997; Winde et al., 2014a, b) and estimating net primary production (Zhang & Quay, 1997; Emerson et al, 1997; Gruber, Keeling & Stocker, 1998; Quay & Stutsman, 2003). Since the surface $\delta^{13}C_{DIC}$ values equilibrate with the atmosphere when waters are ventilated, $\delta^{13}C_{DIC}$ can be used as a proxy for ventilation and indicate water mass types and end-members (Ninnemann & Charles, 1997; Olsen & Ninnemann; 2010;

Mackensen, 2013; Winde et al., 2014a, b; Eide et al, 2017a), as well as used for studying the oceanic Suess Effect (Keeling, 1979; Quay, Tilbrook & Wong, 1992; Gruber et al., 1999; Quay et al., 2003, 2007; Olsen & Ninnemann, 2010).

1.5 Knowledge Gaps

Governing processes of $\delta^{13}C_{DIC}$ signals are considered to be well described for open oceans (Gruber et al., 1999). However, the governing processes of $\delta^{13}C_{DIC}$ in coastal regions are less known compared to the open oceans, since freshwater inputs tend to confound the signals in the coastal regions (Spiker, 1980; Burt et al., 2016b). In order to gain further insight into carbon cycling in coastal regions, the Scotian Shelf water is the focus of our investigation in this study. Various studies have been carried out in Scotian Shelf waters using biogeochemical variables such as DIC, TA, and nitrate, to assess the seasonal variability of DIC and pCO_2 (partial pressure of CO_2), as well as the net community production of the region (e.g., Gatien, 1976; Fournier et al., 1977; Petrie & Drinkwater, 1993; Umoh & Thompson, 1994; Loder et al., 1997; Shadwick et al., 2011; Burt et al., 2013; Shadwick & Thomas, 2014; Burt et al., 2016; Lemay et al., 2018; Rutherford & Fennel, 2018). However, the spatial and seasonal distribution of $\delta^{13}C_{DIC}$ signals and their governing processes on the Scotian Shelf have never been thoroughly researched.

1.6 Thesis Objectives

This project focuses on investigating the temporal and spatial distribution of DIC and $\delta^{13}C_{DIC}$, unraveling their governing processes, as well as quantifying the net primary

production (NCP) from the spring to fall in 2014 throughout the study region. The results of this research aim to deepen the understanding of the inorganic carbon cycling on the Scotian Shelf and to provide a baseline for further studies, for example, with respect to ocean acidification.

The hypotheses in this research are as follows:

1) Concentration of DIC is higher in the mixed layer of Scotian Shelf waters in spring compared to the fall condition, while the $\delta^{13}C_{DIC}$ values gives the opposite result.

2) Biogeochemical processes and freshwater inputs are the dominant processes governing the temporal and spatial variations in the Scotian Shelf waters, compared to other processes such as air-sea exchange, and calcium carbonate dissolution or formation.

3) The metabolic state of the mixed layer in the Scotian Shelf waters in 2014 is autotrophic.

CHAPTER 2. METHODS

2.1 Sample Collection

The discrete bottle samples were collected during April and October cruises of Atlantic Zone Monitoring Program (AZMP) in 2014 on the Canadian Coast Guard Ship Hudson, at stations distributed along four transects on the Scotian Shelf (shown in Fig. 2). These four transects, covering the Scotian Shelf from the southwest to the northeast, were selected to obtain a comparably high resolution view of the shelf waters (Fig. 2). The transects are Browns Bank Line (BBL), Halifax Line (HL), Louisburg Line (LL), and Cabot Strait Line (CSL), with nine, twelve, seven, and six stations sampled along each line respectively (Fig. 2). Samples were collected throughout the water column with a 10-m vertical resolution within the euphotic zone at all stations. The maximum sampling depths for BBL, HL, LL, and CSL are 1890 m, 4718 m, 3774 m, and 469 m, respectively. In this study, only the upper water (above 500 m) in all transects are discussed, as they present the characteristics of shelf water on the Scotian Shelf.

Twelve-liter Niskin bottles mounted on a General Oceanic 24-bottle rosette fitted with a SeaBird CTD (Conductivity Temperature Depth) were used for tapping DIC, $\delta^{13}C_{DIC}$ and TA samples. This allows for the chemical data to be associated with high precision in-situ temperature and salinity data, where the accuracy for temperature and salinity is 0.1 ºC and 0.1, respectively. All DIC and TA samples were poisoned with 100 µL of saturated mercury chloride ($HgCl_2$) to halt any biological activity. All samples were stored in the dark at 4°C to await analysis. The samples were sent to Dalhousie University for DIC and

TA analysis. The $\delta^{13}C_{DIC}$ was analyzed at the Yale Analytical and Stable Isotopic Center (YASIC) of Yale University.

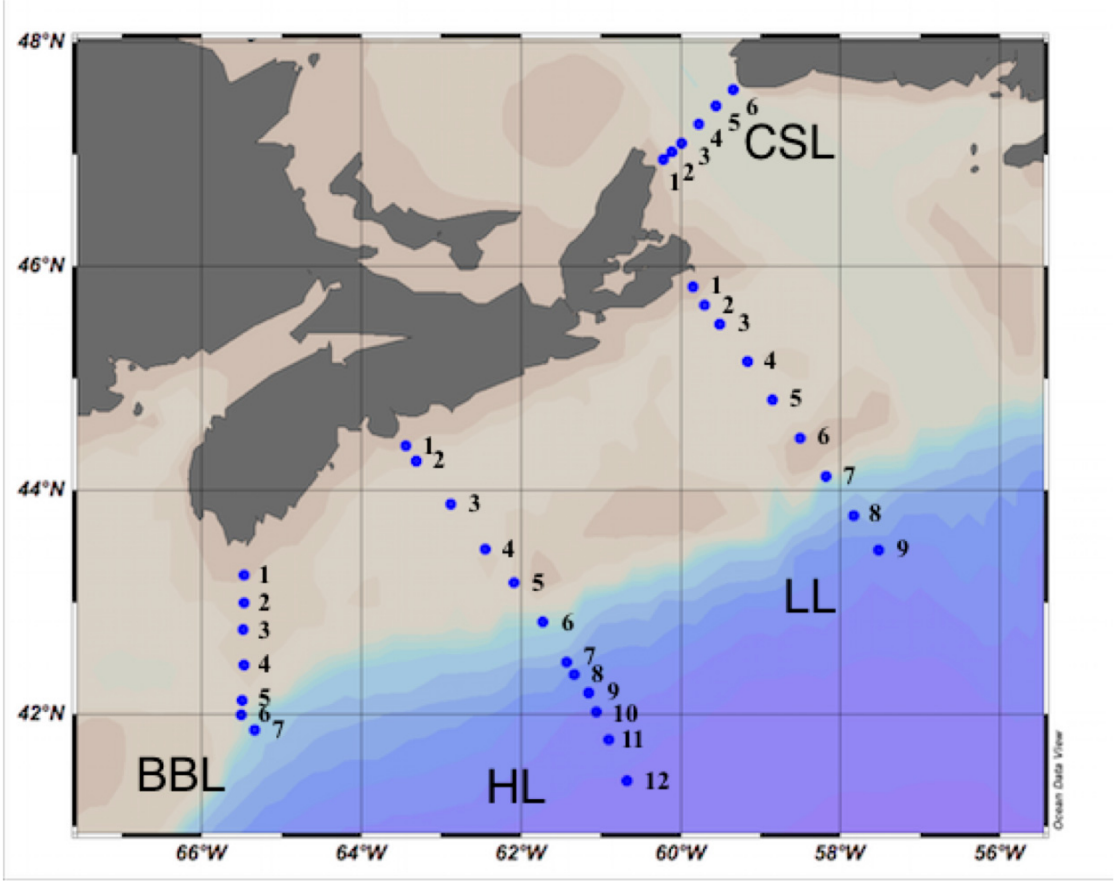

Fig. 2. Sampling locations along four transect lines on the Scotian Shelf. Transects from west to east are Browns Bank Line (BBL), Halifax Line (HL), Louisburg Line (LL), and Cabot Strait Line (CSL), respectively.

2.2 Laboratory Analyses

The carbon isotopic composition of dissolved inorganic carbon ($\delta^{13}C_{DIC}$) was measured by continuous flow-isotope ratio mass spectrometer (CF-IRMS). The instrument used at the Yale University lab was a Thermo Finnigan MAT 253 gas mass spectrometer coupled with a Thermo Electron Gas Bench II via a ConFlo IV split interface. The isotopic ratio is

expressed in per mil (‰) relative to the international Vienna Pee Dee Belemnite (VPDB) standard, where $(^{13}C/^{12}C)_{VPDB}$ is 0.0112372 (Craig, 1957):

$$\delta^{13}C_{DIC}\ per\ mil = \frac{(^{13}C/^{12}C)_{sample} - (^{13}C/^{12}C)_{VPDB}}{(^{13}C/^{12}C)_{VPDB}} \times 1000 \quad (2.1)$$

The reproducibility of the mass spectrometric measurements is 0.1‰VPDB (Craig, 1953), which is used as the uncertainty for all $\delta^{13}C_{DIC}$ values reported here.

2.2.1 Determination of Dissolved Inorganic Carbon (DIC)

DIC and TA were determined using a VINDTA 3C (Versatile Instrument for the Determination of Titration Alkalinity by Marianda), following the standard procedures (Dickson et al., 2007). DIC is determined by coulometric titration. First, a volume of seawater sample from the sample pipette is injected into a stripping chamber which contains phosphoric acid (8.5% H_3PO_4). While the phosphoric acid reacts with the carbonate species from the seawater, CO_2 is being stripped away from the solution by bubbling with a carrier gas (pure N_2). The N_2 gas is supplied directly from a compressed gas cylinder and is passed through a column of soda lime to ensure it does not contain any CO_2. The CO_2 extracted from the seawater sample is then trapped in an absorbent solution containing ethanolamine ($HO(CH_2)_2NH_2$) and a pH-sensitive dye, followed by a titration procedure of the carbamate.

The coulometric titration occurs in a coulometer cell that contains two chambers. The bigger chamber holds a cathode (platinum) and is filled with a cathode solution, which includes ethanolamine (reactive agent), the pH-sensitive dye, and dimethyl sulfoxide ($(CH_3)_2SO$) as solvent. The smaller chamber contains an anode (silver) and is filled with an anode solution, which consists of potassium iodide (KI) in DMSO. Additionally, KI

crystals are added to ensure the potassium iodide remains saturated. The chemical reactions that occur in the coulometer cell are as following:

$$CO_2 + HO(CH_2)_2NH_2 \rightarrow HO(CH_2)_2NHCOO^- + H^+ \quad (2.2)$$

$$H^+ + OH^- \rightarrow H_2O \quad (2.3)$$

As the cathode solution is acidified, the color of the dye changes correspondingly. The electrolysis of water in the cathode generates OH^- (equation 2.4), which is used to titrate the hydroxyethylcarbamic acid. In the meantime, silver is oxidized in the anode (equation 2.5).

$$H_2O + e^- \rightarrow \frac{1}{2} H_{2(g)} + OH^- \quad (2.4)$$

$$Ag_{(s)} \rightarrow Ag^+ + e^- \quad (2.5)$$

Since the number of electrons needed to produce OH^- to neutralize the solution can be measured by the coulometer, the concentration of DIC in μmol/kg can be obtained according to Faraday's second law.

2.2.2 Determination of Total Alkalinity (TA)

Seawater sample is injected into an open titration cell, which is connected to a water bath to maintain the temperature of the sample at 25°C. Doses of 0.15 mL (0.1 molkg^{-1}) hydrochloric acid (HCl) solution are delivered to the titration cell by a piston burette, which is controlled by the computer. During the titration, continuous measurements of the evolution of the potential between the pair of electrodes were taken to monitor the progress of titration. Total alkalinity is then computed by the VINDTA LabView software using a modified Gran approach (Dickson et al., 2007).

2.2.3 Calibration with Reference Material

The Certified Reference Materials (CRMs) are 500 mL volumes of seawater with predetermined DIC concentrations and TA, provided by A. G. Dickson et al. (Scripps Institution of Oceanography) (2007). The CRMs are analyzed at the beginning and the end of each sample measurement period, using the methods above. The resulting values of DIC and TA are used as a baseline to calibrate our sample measurements. This routine CRMs analysis ensures that the uncertainties of DIC and TA measurements are less than 2 μmolkg $^{-1}$ and 3 μmolkg $^{-1}$, respectively.

2.3 Determination of the Biological Component of DIC (DIC_{bio})

Air-sea gas exchange, biological production and consumption of organic material, and pelagic calcium carbonate formation and dissolution, all have influences on DIC concentrations in water. In order to isolate the biological component of DIC (DIC_{bio}), the surface DIC concentration at atmospheric equilibrium (DIC_{pCO2}) is subtracted from the observed DIC (DIC_{obs}), see equation 2.6:

$$DIC_{bio} = DIC_{obs} - DIC_{pCO2=399.75} \quad (2.6)$$

The atmospheric equilibrium value of 399.75 μatm was the average atmospheric pCO_2 between April (404.05 μatm) and October (395.46 μatm) of 2014, obtained from the Mace Head atmospheric station in Ireland. DIC_{pCO2} values were calculated using the CO_2Sys program of Lewis and Wallace (1998). The difference between $DIC_{pCO2=404.05}$ and $DIC_{pCO2=395.46}$ is approximately 3.2 μmol/kg, which is insignificant compared to the range of values calculated in this study. Therefore, $DIC_{pCO2=399.75}$ is used when calculating DIC values at atmospheric equilibrium. This method assumes that any excess or deficit relative

to $DIC_{pCO2=399.75}$ is mainly due to the biological production/consumption of organic matter. The temperature change in the water can alter the pCO_2 value in the surface water and thus affect the $DIC_{pCO2=399.75}$ term. The temperature effect on ocean-surface-water pCO_2 is in the range of ±4 % $°C^{-1}$ (Takahashi et al.,1993), which leads to a change of only about 6 µmol/kg in DIC_{bio} with a 1ºC change in temperature. In order to minimize the temperature impact on surface DIC_{bio}, we computed DIC_{bio} separately for each season, yielding consistent estimates for each respective season. In this method, we assume that the surface water temperature does not vary or varies only incrementally within the observational window. Lastly, the dissolution and formation of $CaCO_3$ are considered to be in steady-state in the well-mixed surface waters of the Scotian Shelf. Therefore, another assumption of this method is that the influence of formation or dissolution of $CaCO_3$ is negligible in the Scotian Shelf waters.

DIC_{bio} is calculated as a relative value, only the relative change in its magnitude is considered, rather than the magnitude of any particular value itself. Given the above assumptions, an increase in DIC_{bio} indicates the production of DIC by respiration of organic matter, while a decrease of DIC_{bio} indicates the consumption of DIC during photosynthesis.

CHAPTER 3. RESULTS AND DISCUSSION

3.1 Seasonal Variability of Temperature and Salinity

The seasonal variability of temperature and salinity regulates the structure of the water column on the Scotian Shelf. The seasonal variation of stratification in the Scotian Shelf water is exhibited in Figs. 3 and 4. The seasonal variability of sea-surface temperature is the strongest in the northwest Atlantic compared to any region in the Atlantic between 30 ºS and 70 ºN (Weare & Newell, 1977). Our observations in the Scotian Shelf waters from April and October yielded a range of sea-surface temperature about 25 °C (-1.2 °C to 24.6 °C). This large seasonal amplitude of surface water temperature is considered to be a well-documented feature of the northwestern Atlantic shelf (e.g., Weare & Newell, 1977; Umoh & Thompson, 1994). The seasonal variation in temperature on the Scotian Shelf is primarily controlled by the surface heat flux, with mixing, horizontal advection, and diffusion playing minor roles (Umoh & Thompson, 1994). The temperature generally decreases shoreward and with depth in both seasons (Figs. 3 and 4). In the spring, the Cabot Strait Line exhibited the coldest mean surface temperature compared to other transects, due to the outflow water from the seasonally ice-covered Gulf of St. Lawrence (Fig. 3). In the fall, the warmest temperature was found in the surface water and the coldest temperatures were found at about 50 to 100 m depth, close to the shore (Fig. 4). The isotherms are relatively flat at the outer shelf (Fig. 4). In the case of Cabot Strait Line, the relatively warm freshwater mixture flows out of the CSL along the coast of Nova Scotia and the relatively cold Labrador current flows into the CSL along the shore of

Newfoundland. As a result, the nearshore (close to Nova Scotia) area of the CSL exhibits higher temperature than the offshore area (close to Newfoundland) in the fall (Fig. 4).

In winter and early spring, a two-layer system is formed on the shelf. The upper 70-100 meters of the water column are well-mixed and dominated by cold and relatively fresh water, while the deeper part of the water column is warmer and relatively saline slope water (Fig. 3). In summer and fall, the water column is well stratified, and a three-layer system is present (Fig. 4). The surface water (upper 30 meters) is composed of warm freshwater and is strongly influenced by the riverine input from the Gulf of St. Lawrence. The peak of this river input occurs from June to October, and as a result, generates an inner shelf flow (NSC), which possesses salinities that generally range from 30 to 33 and decreases the surface salinity on the Scotian Shelf (Fig. 4) (Fournier et al., 1977; Loder et al., 1997). Underlying this surface water is a cold intermediate layer (CIL) that extends to about 70-100 meters in depth. Beneath the CIL is the warmer and more saline slope water, which increases its salinity monotonically with depth (Fig. 4). Salinity on the Scotian Shelf increases with the distance offshore due to the influence of the northward transport of the Warm Slope Water. Together with the influences from the freshwater input and the WSW, the surface salinity on the Scotian Shelf ranges from 28.7 to 36. This large salinity variability is also observed by Shadwick in 2010 (her salinity observations ranged from 30 to 36). The seasonal variations in the distributions of DIC and $\delta^{13}C_{DIC}$ in Scotian Shelf water can be partially explained by the difference in stratification in the water column between spring and fall. This will be discussed in subsequent sections.

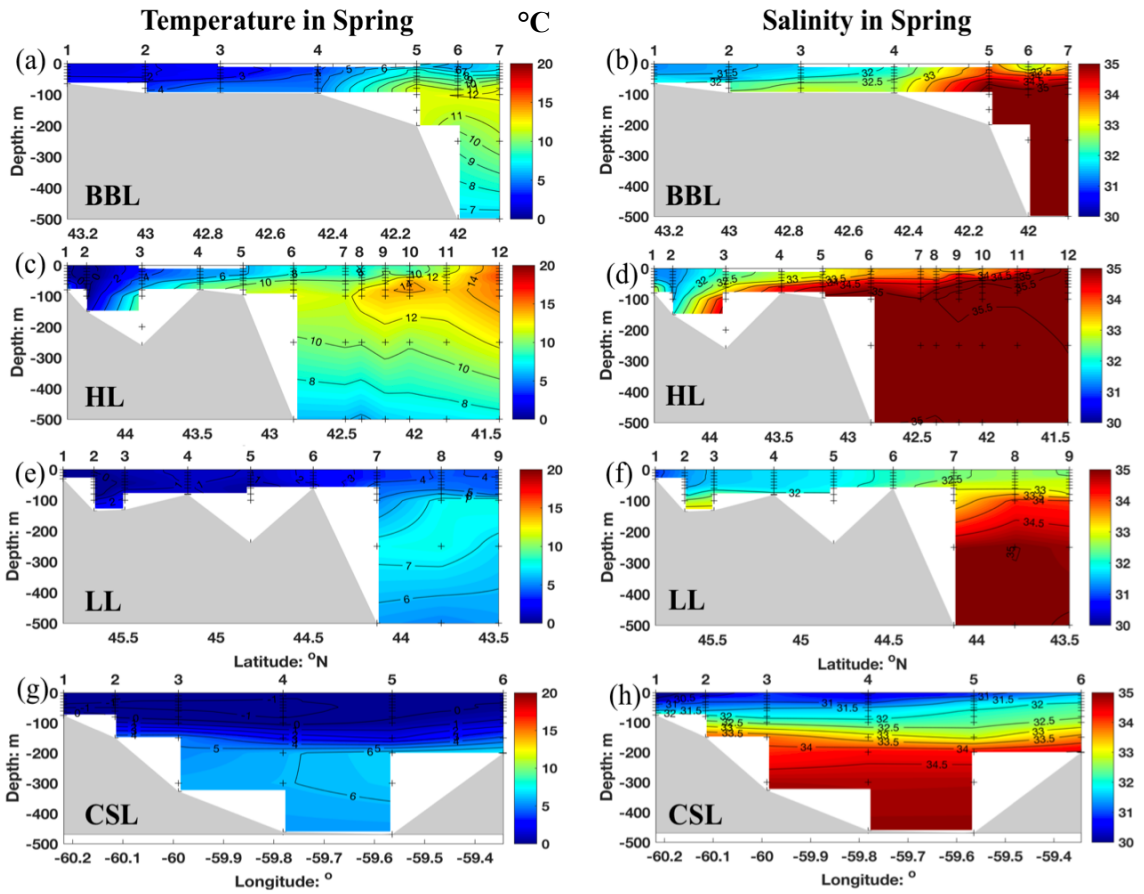

Fig. 3. Temperature (°C) and salinity distributions along Browns Bank line, Halifax line, Louisburg line, and Cabot Strait line in April 2014.

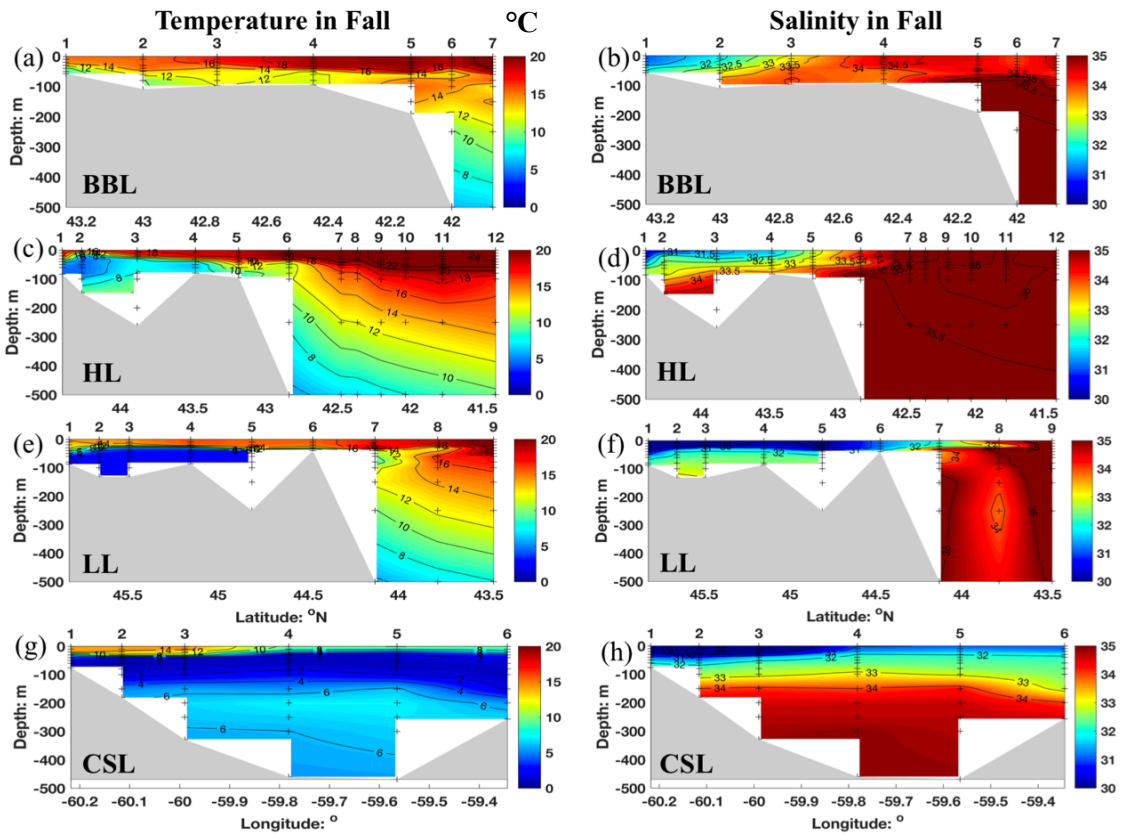

Fig. 4. Temperature (°C) and salinity distributions of Browns Bank line (BBL), Halifax line (HL), Louisburg line (LL), and Cabot Strait line (CSL) in October 2014.

3.2 Spatial Variability of DIC and $\delta^{13}C_{DIC}$

3.2.1 Browns Bank Line

In spring, the mean surface DIC concentration on BBL is 2053 ±26 µmol/kg, with the lowest values of surface DIC concentrations on the order of 2029 µmol/kg, was found in the surface of nearshore station (BBL 3) (Fig. 5). The mean surface $\delta^{13}C_{DIC}$ value along BBL is 0.9 ±0.1 ‰VPDB, with a maximum value of 1.2 ‰VPDB found at offshore station 6. In the subsurface, the lowest DIC concentration on the order of 2060 µmol/kg was found in the nearshore station, BBL 1. At station 4 and 5, the DIC concentrations at a 100 m depth reached 2130 µmol/kg and the values continue to increase in deeper depths at BBL

6 and 7, approaching a value of 2172 µmol/kg. $\delta^{13}C_{DIC}$ values in the subsurface ranged from 0.3 ‰VPDB to 0.9 ‰VPDB with an average value of 0.6 ±0.1 ‰VPDB. The DIC concentrations and $\delta^{13}C_{DIC}$ values stays homogenously in the deeper water at offshore stations, with a mean value of 2162 ±21 µmol/kg and 0.6 ±0.1 ‰VPDB, respectively (Fig. 6).

In fall, the surface DIC concentrations at all stations were reduced compared to spring values ($p<0.05$), in which the most pronounced reduction in concentrations was seen at nearshore stations (BBL 1 and 2) and the offshore station BBL 7 (compare Figs. 5 and 7). The DIC concentrations at the surface extended from a minimum value of 1946 µmol/kg (at station 1 closest to the shore) to 2045 µmol/kg (at station 3). The average surface DIC concentration and average $\delta^{13}C_{DIC}$ values were 2004 ±26 µmol/kg and 1.3 ± 0.2 ‰VPDB, respectively. The highest $\delta^{13}C_{DIC}$ value on the order of 1.6 ‰VPDB was observed at nearshore stations 1 and 2, and the values decreased further offshore (Fig. 8). In comparison to spring conditions, $\delta^{13}C_{DIC}$ values at the surface increased at all stations along BBL ($p<0.05$), due mainly to the biological production processes dominating in the fall. In subsurface waters, the average DIC concentration and $\delta^{13}C_{DIC}$ value are 2080 ± 42 µmol/kg and 0.8 ±0.3 ‰VPDB, respectively. The DIC concentrations keep increasing in the deeper waters at offshore stations and reach an average value of 2168 ± 19 µmol/kg. Reciprocally, the $\delta^{13}C_{DIC}$ values in the deep waters decreases to an average value of 0.5 ±0.2 ‰VPDB.

3.2.2 Halifax Line

The distribution of DIC and $\delta^{13}C_{DIC}$ in Halifax Line showed similar patterns to the Browns Bank Line. In spring, the mean surface concentration of DIC was 2052 ±26 μmol/kg, with minimum values on the order of 2002 μmol/kg found at nearshore stations HL 1 and 2 and with maximum values on the order of 2105 μmol/kg observed at offshore stations 11 and 12 (Fig. 5). The surface mean $\delta^{13}C_{DIC}$ value along the Halifax Line was slightly higher than it was on the BBL by 0.1 ‰VPDB, with a value of 1.0 ‰VPDB (Fig. 6). The maximum $\delta^{13}C_{DIC}$ along the HL was 1.3 ‰VPDB, observed at station 1; this value was also 0.1 ‰VPDB higher than the maximum value found on the BBL. In the subsurface waters, the average DIC concentrations were higher than on the BBL, with the lowest values found in nearshore stations and increasing further offshore. The maximum subsurface DIC concentration was found at HL 12 with a value of 2131 μmol/kg. The $\delta^{13}C_{DIC}$ values in subsurface waters was 0.6 ± 0.2 ‰VPDB with a minimum value of 0.3 ‰VPDB found at nearshore station HL 3. The highest DIC concentrations were observed at deep waters with a mean value of 2176 ± 30 μmol/kg. Comparably low $\delta^{13}C_{DIC}$ values were also observed in the deep waters.

In fall, the surface DIC concentrations at all stations along Halifax Line were reduced relative to spring values ($p<0.05$). To be exact, the mean surface DIC concentrations in the Halifax Line were lower than observed in spring by 49 μmol/kg ($p<0.05$), with a value of 2003 ±43 μmol/kg. The surface DIC concentrations ranged from a minimum value of 1916 μmol/kg observed at nearshore (HL 2) to a maximum value of 2046 μmol/kg shown at offshore stations HL 11 and 12 (Fig. 7). The average value of surface $\delta^{13}C_{DIC}$ in the fall was 1.3 ± 0.2 ‰VPDB, which was higher than the value obtained in the spring by 0.3 ‰VPDB ($p<0.05$). At station HL 3 and 4, the maximum value of $\delta^{13}C_{DIC}$ (2.0 ‰

VPDB) was observed. This was the highest $\delta^{13}C_{DIC}$ value among all transacts in both seasons (Fig. 8). In the subsurface waters, the DIC concentrations are higher relative to values on the Browns Bank Line, while the subsurface $\delta^{13}C_{DIC}$ values were comparably lower (Figs. 7 and 8). The subsurface $\delta^{13}C_{DIC}$ values were lower at nearshore and increased offshore ($p<0.05$). The lowest values of $\delta^{13}C_{DIC}$ were observed in deep waters, with an average value of 0.5 ± 0.2 ‰ VPDB.

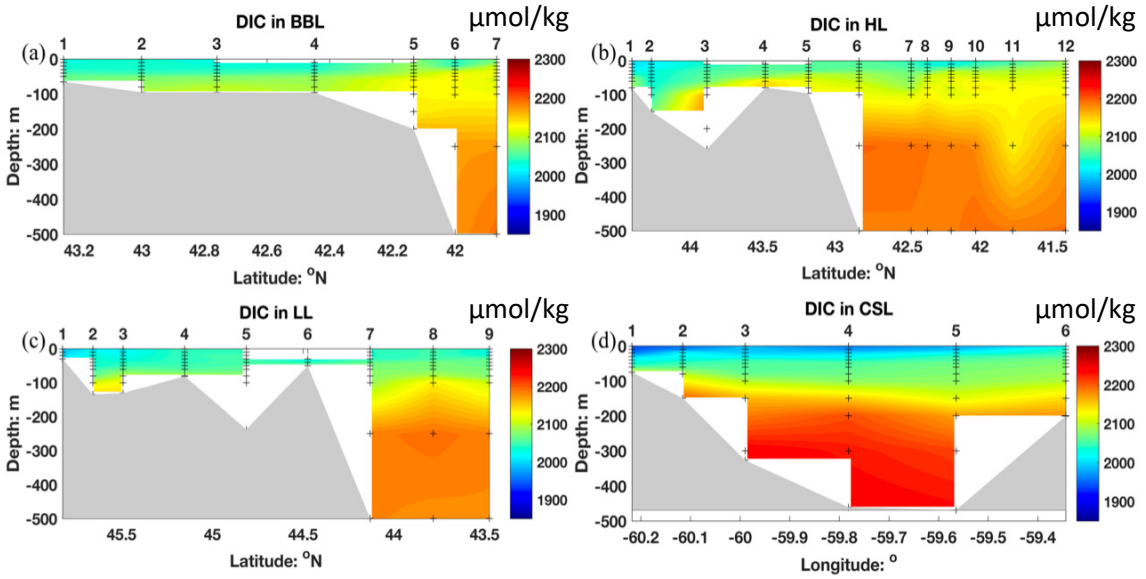

Fig. 5. Distribution of DIC concentrations (µmol/kg) in all transects in April 2014.

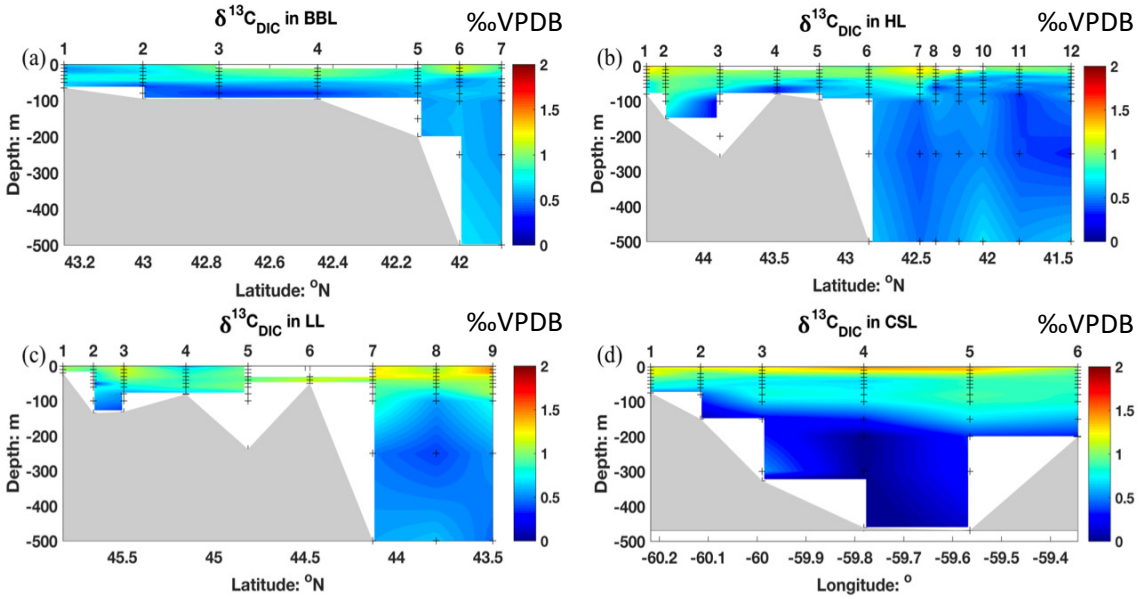

Fig. 6. Distribution of $\delta^{13}C_{DIC}$ values (‰VPDB) in all transects in April 2014.

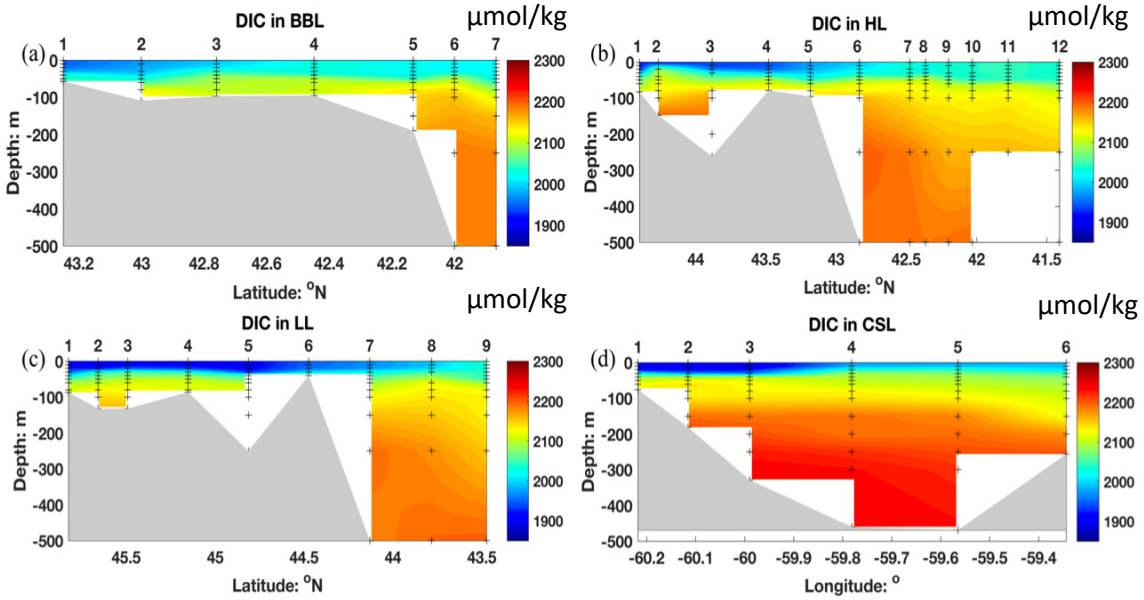

Fig. 7. Distribution of DIC concentrations (µmol/kg) in all transects in October 2014.

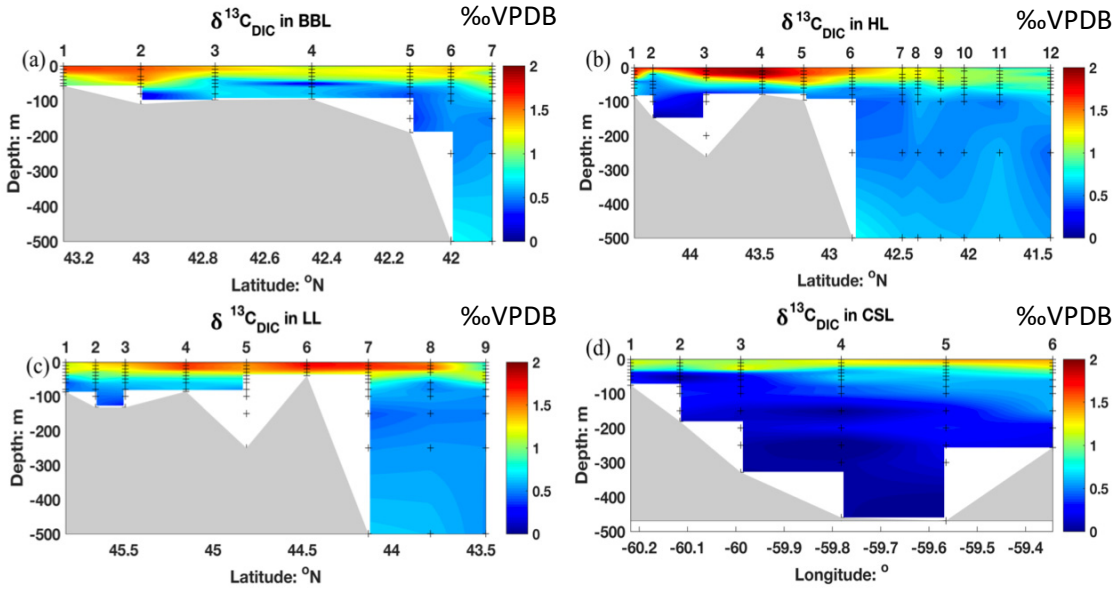

Fig.8. Distribution of $\delta^{13}C_{DIC}$ values (‰VPDB) in all transects in October 2014.

3.2.3 Louisburg Line

Similarly to the Browns Bank Line and Halifax Line, seasonal variability of DIC and $\delta^{13}C_{DIC}$ were also observed in the stations along Louisburg Line. In spring, the surface mean DIC concentration was 2033 ±17 µmol/kg, which was about 20 µmol/kg lower than the mean values observed in both BBL and HL. The minimum surface DIC is 1987 µmol/kg and was observed at LL1, the most nearshore station, while the maximum surface DIC (2060 µmol/kg) was observed at offshore stations LL 8 and 9. The average surface $\delta^{13}C_{DIC}$ values along LL was 1.1 ‰VPDB, with the maximum value on the order of 1.5 ‰VPDB observed at offshore station LL 9. This value is also higher than the maximum values observed in HL and BBL in the surface waters. Subsurface DIC concentrations were slightly lower relative to values on HL and BBL, while $\delta^{13}C_{DIC}$ values in subsurface waters revealed the opposite trend ($p<0.05$).

In fall, surface DIC concentrations were lower at all stations along the Louisburg Line relative to concentrations in the spring condition ($p<0.05$). The mean surface DIC concentration of LL was 1962 ±52 µmol/kg, which was also lower than the mean values obtained on BBL and HL. Again, the lowest DIC concentration was observed at the nearshore station LL 1 and 2, with a value of 1900 µmol/kg. Higher concentrations were found offshore with the maximum value on the order of 2051 µmol/kg observed at the furthest station from shore (LL 8). The $\delta^{13}C_{DIC}$ value at the surface ranged from 0.8 ‰VPDB to 1.7 ‰VPDB with a mean value of 1.4 ± 0.2 ‰VPDB. The lowest values were observed at LL 1 and LL 9, and the maximum values were observed at LL 6 and LL 7. Subsurface DIC concentrations and $\delta^{13}C_{DIC}$ values in Louisburg Line closely resemble those observed in BBL and HL.

3.2.4 Cabot Strait Line

As mentioned in section 2, in the surface of CSL, the Labrador Shelf water flows into the Gulf of St. Lawrence (GSL) along the eastern side of the Cabot Strait, while the St. Lawrence Estuary water flows out of the GSL along the western side of the Cabot Strait. Beneath the surface is the cold intermediate layer which extends to about 70 to 100 m. Water within the deeper depths originates from the south and flows into the Cabot Strait through the Laurentian Channel. Due to the location of Cabot Strait Line, the distributions of DIC and $\delta^{13}C_{DIC}$ in CSL were somewhat different from those found in HL, BBL, and LL. In spring, the mean surface DIC concentration was 1997 ±32 µmol/kg, which was the lowest value relative to the values observed at HL, BBL, and LL. The minimum value observed was 1939 µmol/kg, found at a nearshore station (CSL 1, closest to the Nova

Scotia side of the strait). The maximum value was approximately 2054 µmol/kg and was observed at the offshore station (CSL 6, close to the Newfoundland side of the strait). The average surface $\delta^{13}C_{DIC}$ value in the spring on the CSL reached 1.1 ±0.1 ‰VPDB and was the highest value among those observed at other transects. The maximum surface $\delta^{13}C_{DIC}$ value on the CSL was 1.5 ‰VPDB, observed at offshore stations 4 and 5. In the subsurface waters, the water was well mixed in spring at all stations along the CSL. The mean DIC concentration and $\delta^{13}C_{DIC}$ value in the subsurface was 2065 ± 21 µmol/kg and 0.8 ±0.1 ‰VPDB, respectively.

In fall, the surface DIC concentrations ranged from 1882 µmol/kg (observed at CSL 3) to 2090 µmol/kg (observed at CSL 4), with an average value of 1967 ± 62 µmol/kg. The average surface $\delta^{13}C_{DIC}$ value was 1.1 ± 0.1 ‰VPDB. Unlike HL and BBL, the maximum value on the order of 1.4 ‰VPDB was observed at offshore (the side close to Newfoundland) station CSL 6. This anomaly could indicate the influence of river input on the Cabot Strait, which decreases the surface $\delta^{13}C_{DIC}$ value at nearshore (the side close to the Scotian Shelf) stations along CSL. In the subsurface, the lowest $\delta^{13}C_{DIC}$ values were found nearshore, increasing with distance from the shore. The mean $\delta^{13}C_{DIC}$ value observed in the deeper waters of CSL (>100 m) was 0.1 ±0.1 ‰VPDB, which was the lowest compared to $\delta^{13}C_{DIC}$ values found in the deeper waters along other transects. These low values of $\delta^{13}C_{DIC}$ are a result of the water originating from the South, being rich in DIC, and having old biological history.

3.2.5 Shelf-Wide Patterns

Spatial variability of DIC and $\delta^{13}C_{DIC}$ along the Scotian Shelf was observed in both the spring and fall of 2014. These two seasons showed similar shelf-wide patterns in DIC and $\delta^{13}C_{DIC}$ distributions, while the observations in the spring showed less variability, thus for simplification, only the data observed in the fall was illustrated for depicting the spatial distribution of DIC and $\delta^{13}C_{DIC}$ in the region. The spatial variability was examined from three aspects: alongshore, cross-shelf and with depth.

Spatial Variability Alongshore (from the Gulf of St. Lawrence to the Gulf of Maine)

As shown in Fig. 7, in the nearshore surface water, the mean DIC concentration was the lowest at CSL (1967 ± 62 μmol/kg). The value increased along the shelf and reached the highest mean surface DIC concentration at BBL (2004 ± 26 μmol/kg). At all stations, the maximum $\delta^{13}C_{DIC}$ values were observed in surface water (Fig. 8). The highest $\delta^{13}C_{DIC}$ value in BBL was observed at BBL 1 and BBL 2, while in the case of Halifax Line, it was observed at HL 3 and HL 4 (Fig. 8). Along the Louisburg Line, the maximum $\delta^{13}C_{DIC}$ values were found at LL 6 and LL 7 and at CSL 6 along the Cabot Strait Line (Fig. 8). The distribution of DIC and $\delta^{13}C_{DIC}$ reveals the influence of the freshwater input from the Gulf of St. Lawrence (Figs. 4, 7 and 8). This effect was strongest in CSL and weakened along the flowing direction towards BBL. The relationship between $\delta^{13}C_{DIC}$ and DIC in fall along the four transects as well as observations from the Gulf of St. Lawrence is presented in Fig. 9. Observations from the Gulf of St. Lawrence were provided by Alfonso Mucci, obtained from a 2016 cruise in May, in order to help explain the distribution of selected variables along other transects on the Scotian Shelf. The surface water exhibited the highest $\delta^{13}C_{DIC}$ values and lowest DIC concentrations, partly as a result of the

photosynthesis process preferentially taking up light carbon. The highest values of $\delta^{13}C_{DIC}$ among all observations were seen at station 3 and 4 along the Halifax Line (Figs. 8 and 9). As seen in Fig. 9, the red arrow indicates the inner shelf flow (Nova Scotia Current), while the green arrow illustrates the shelf break flow, which flows out from the southwest side of CSL (the side near Nova Scotian coast) and moves along the shelf break towards the Gulf of Maine. As shown in Fig. 9, there is a strong negative relationship between DIC and $\delta^{13}C_{DIC}$ in the shelf waters. However, the relationship between $\delta^{13}C_{DIC}$ and DIC from the surface waters of CSL and LL (where the red arrow indicates) does not fit in this negative slope. Rivers are often depleted in $\delta^{13}C_{DIC}$ due to the dissolution of biogenic carbon in soils (Spiker, 1980). The drawdown of $\delta^{13}C_{DIC}$ values in the surface water of CSL and LL can be explained by the influence of riverine input, which in turn leads to a positive relationship between $\delta^{13}C_{DIC}$ and DIC in the inner shelf flow.

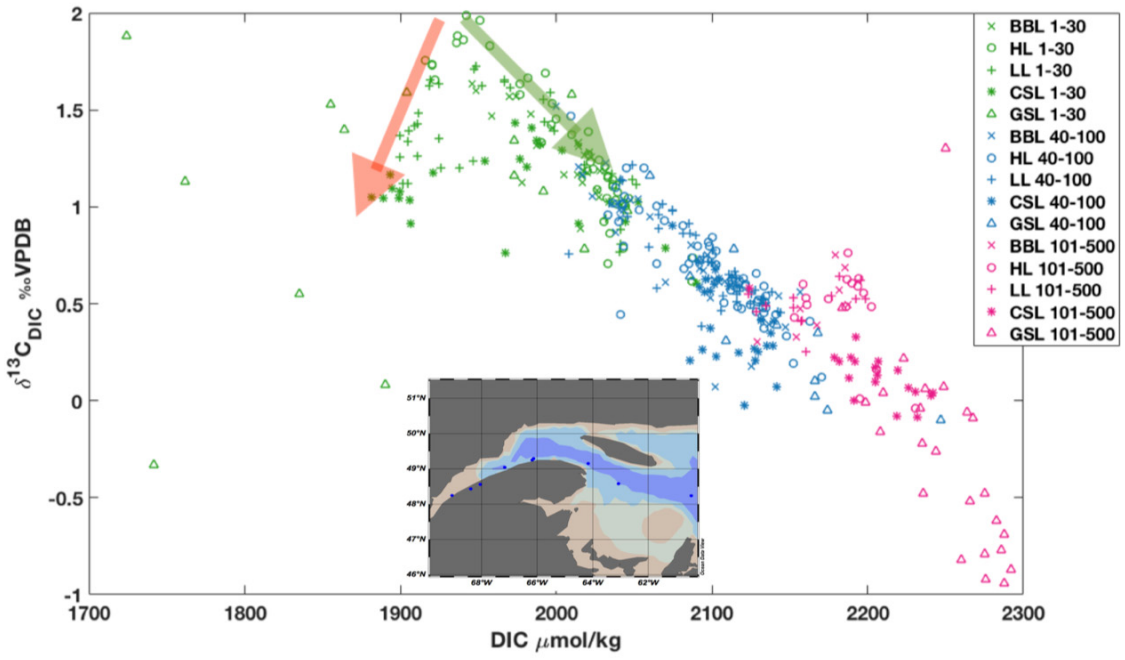

Fig.9. $\delta^{13}C_{DIC}$ vs. DIC in the fall of 2014. Different colors indicate water samples collected from different water depths (green: surface water 1-30m; blue: 40-100m; hot pink: 101-500m). The five

different shapes represent water samples from five different transects ("x," "o," "+," "*," and "Δ" indicate BBL, HL, LL, CSL, and samples from Gulf of St. Lawrence, respectively). The red and green arrows indicate the NSC and the shelf break flow, respectively. The samples were obtained from a 2016 cruise in May in the Gulf of St. Lawrence (GSL), from the middle of the Lower St. Lawrence Estuary to the southern tip of Anticosti Island in the Gulf of St. Lawrence (shown in the topography). This data is provided by Alfonso Mucci from McGill University (pers. comm.).

Spatial Variability Cross-shelf

The cross-shelf variability of DIC and $\delta^{13}C_{DIC}$ for the four transects was observed in both the spring and fall of 2014. The surface DIC concentrations rise with increasing distance offshore (Fig. 7), which is consistent with the study conducted by Shadwick and Thomas in 2014. As mentioned above, the locations of maximum $\delta^{13}C_{DIC}$ values vary among the four transects, due to different degrees of influences received from the freshwater input. Shadwick (2010) also reported that the salinity increases further offshore due to the northward transport of the Gulf Stream water; the surface temperature follows the same pattern. This is reflected in our results as well (see Figs. 3 and 4). The freshwater input has a dominant control on nearshore surface water, while the offshore water is mainly affected by the Warm Slope Water, which is modified by the oceanic water from the Gulf Stream; this leads to the patterns of variability of DIC and $\delta^{13}C_{DIC}$ observed from our results.

Spatial Variability with Depth

The variability of DIC and $\delta^{13}C_{DIC}$ was also observed throughout the water column on the Scotian Shelf. During the productive season, the surface DIC decreased to a minimum due to phytoplankton uptake and freshwater dilution (see also Shadwick et al., 2011). DIC concentrations in subsurface waters increase as a result of respiration of sinking organic

matters. In the deep water, DIC values tend to increase or stay constant (Figs. 7 and 9) due to the influence of mixing with the Warm Slope Water.

$\delta^{13}C_{DIC}$ values, on the other hand, show an opposite trend compared to DIC distributions. In the surface water, $\delta^{13}C_{DIC}$ reached a maximum value due to biological production through photosynthesis. Subsurface $\delta^{13}C_{DIC}$ decreased to minimum values then slightly increase or stay constant in the deeper water (Figs. 8 and 9). This observation in deep water is true except in the case of CSL. The $\delta^{13}C_{DIC}$ values measured in the deep water of CSL were lower than the values found in the subsurface waters; in fact, they exhibited the lowest $\delta^{13}C_{DIC}$ values in the Scotian Shelf waters. The deep water in CSL is a mixture of Labrador Current and North Atlantic Central waters, abundant in DIC, deficient in oxygen with old biological history (Gilbert et al., 2005; Mucci et al., 2011), therefore exhibiting extremely low $\delta^{13}C_{DIC}$ values.

3.3 Seasonal Variability of DIC and $\delta^{13}C_{DIC}$

The different species of the carbonate system such as pCO_2, pH, DIC, and $\delta^{13}C_{DIC}$ respond to changes in environmental conditions, both biotically and abiotically at different time scales. While pH and pCO_2 respond on relatively short time-scales (hours to days) (e.g., Vandemark et al., 2011; Thomas et al., 2012; Craig et al., 2014; Lemay et al., 2018), changes in DIC and $\delta^{13}C_{DIC}$ reflect processes at monthly to seasonal time scales (e.g., Mook, Bommerson & Staverman, 1974; Broecker & Peng, 1974; Keeling, 1979； Lynch-Stieglitz et al., 1995； Shadwick et al., 2011; Schmittner et al., 2013). Alkalinity in contrast generally responds at a much longer time scale, possibly with the exception of anaerobic metabolic processes (e.g., Thomas et al., 2009). We exploit these characteristics

regarding DIC and $\delta^{13}C_{DIC}$ in order to unravel seasonal changes. As such, our April observations of DIC and $\delta^{13}C_{DIC}$ constitute winter observations, integrating fall and winter processes until just before the onset of the spring bloom. Accordingly, our fall observations integrated over the productive period during spring and summer and reveal, ideally, the maximum extent of the biological impact on the system. An analogous situation might be seen in temperature, where the minimum temperature marks the onset of spring (or end of winter), and the maximum temperature marks the end of summer or the onset of fall.

The relationships between total alkalinity and DIC as a function of salinity in the Scotian Shelf waters in spring and fall of 2014 are shown in Fig. 10. Salinity values on the shelf ranged from 28.7 to 36.4, with the maximum salinity found in deeper water at offshore stations (HL 11 and 12), and the minimum value found in surface water from the nearshore stations of Cabot Strait (CSL 3).

TA concentrations varied from 2030 µmol/kg to 2406 µmol/kg. There is a strong positive relationship between TA and salinity in both seasons, where TA = 45.5 (±0.5) × Sal + 1204 (±21), R^2=0.97, Fig. 10). Since a one unit change in $CaCO_3$ concentration would lead to a two unit change in TA and a one unit change in the DIC concentration, this conservative relationship between TA and salinity again supports the assumption that calcium carbonate dissolution or formation can be considered a minor factor of controlling the inorganic carbon cycling in this region.

DIC concentrations extend from a minimum value of 1881 µmol/kg to a maximum value of 2242 µmol/kg, with the lowest values corresponding to the lowest salinity in the water. The relationship between DIC and salinity in Fig. 10 also indicates that 86% of the variability in DIC is due to changes in salinity (DIC = 31.74 (±7.4) × Sal + 1006 (±241),

R^2=0.86, where the DIC concentrations were averaged into 0.5 bins of salinity and the least square linear regression was performed on these bin averaged results). Generally, the DIC concentration increases with increasing salinity and there is more variability in the relationship between DIC and salinity in fall than in spring due to the absence of biological activity in spring (Fig. 10).

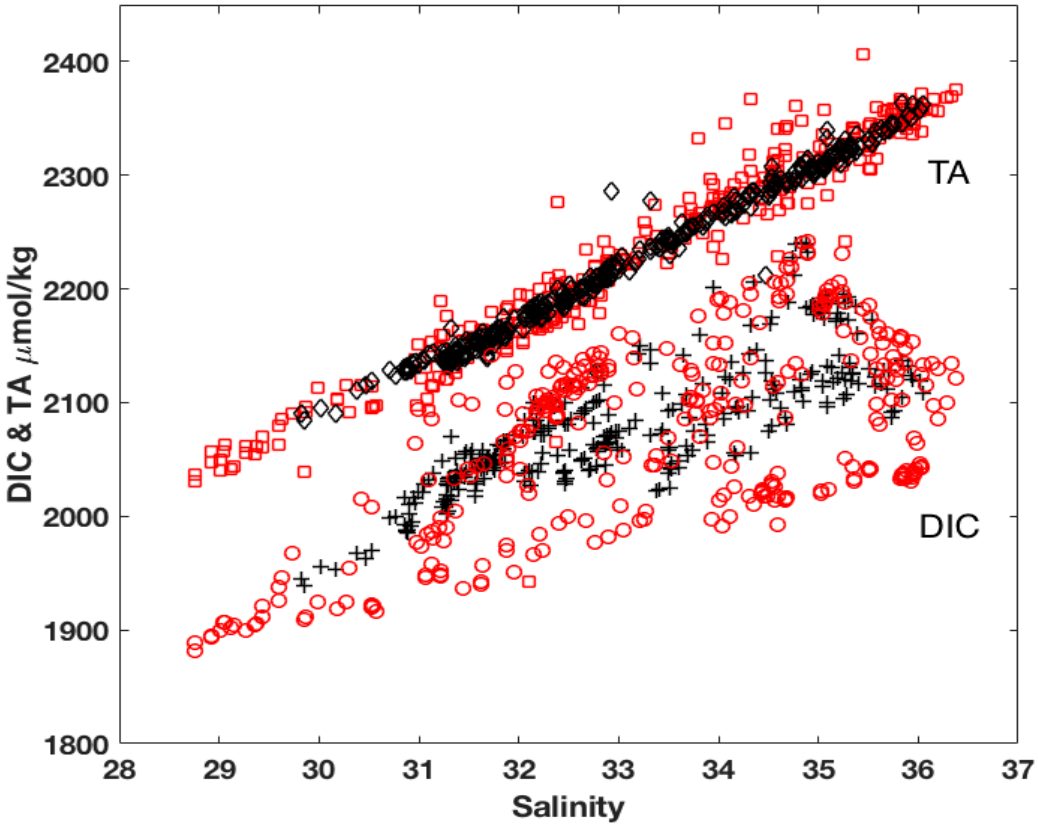

Fig. 10. TA and DIC as a function of salinity for all stations were observed in spring (black) and fall (red) in 2014 cruise. Diamond and square shapes represent TA while circle and plus sign shapes stand for DIC.

Given the integration of time scales of DIC and $\delta^{13}C_{DIC}$ being discussed above, the seasonal variability of DIC and $\delta^{13}C_{DIC}$ in the fall and spring can be depicted clearly (shown in Fig. 11). In the fall, the DIC concentrations and $\delta^{13}C_{DIC}$ values range from 1881

to 2242 μmol/kg and -0.1 to 2.0 ‰VPDB, respectively. This comparably wide range of values in the fall indicates underlying mechanisms, which includes river input, photosynthesis and respiration processes. As mentioned before, the fall observations integrated over the most productive period exhibit the maximum extent of the biological impact on the system. As a result, the highest $\delta^{13}C_{DIC}$ values associated with low DIC values are found in the surface water in fall. To be explicit, since marine primary producers preferentially take up light carbon (^{12}C) when assimilating the dissolved organic carbon from seawater into organic carbon during photosynthesis (O'Leary, 1988) and leave the heavier ^{13}C behind in the water, the $\delta^{13}C_{DIC}$ values in results increase, and DIC values decrease. This explains the peak of $\delta^{13}C_{DIC}$ values observed in fall (Fig. 11). Reciprocally, respiration of organic matter releases light carbon into seawater thereby increasing DIC values while $\delta^{13}C_{DIC}$ values decrease. Since the shelf water is well stratified in fall, surface water exhibits minimum DIC concentrations and maximum $\delta^{13}C_{DIC}$ values throughout the water column due to photosynthesis; maximum DIC concentrations and minimum $\delta^{13}C_{DIC}$ values appear in subsurface water, as a result of respiration of organic matter (see Fig. 12). In summer and fall, the Scotian Shelf receives freshwater from the Gulf of St. Lawrence through the Cabot Strait (Loder et al., 1997). The observations where DIC values lie between 1880 and 1920 μmol/kg reflect the influence from freshwater inputs on the shelf, as the freshwater dilutes the DIC concentrations in the surface water, leading to low DIC values with relatively low $\delta^{13}C_{DIC}$ values in the observation.

In spring, signals of biological production in surface water "vanished" (Fig. 11). No observations of particularly high values of $\delta^{13}C_{DIC}$ associated with low DIC values were observed. One of the reasons is that the respiration of organic matter dominates over

production until spring. Therefore, the more light-carbon released into water, the higher DIC concentrations and the lower $\delta^{13}C_{DIC}$ values are found. The second reason relates to the hydrogeological characteristics of the Scotian Shelf. In winter and early spring, the ice formation on the Gulf of St. Lawrence prevents the Scotian Shelf from receiving freshwater from the Gulf, meaning that river dilution does not occur in the winter or spring. Additionally, surface water is well mixed during these seasons (winter and spring) due to convection and wind mixing (Shadwick & Thomas, 2014). Due to a combined effect of respiration of organic matter and the mixing of carbon-rich water from below, the surface DIC concentration is higher in the spring than in the fall (Fig. 12).

Seasonal variability of distributions of DIC and $\delta^{13}C_{DIC}$ values in the Scotian Shelf water are evident between spring and fall, where in general, more variability is exhibited in the fall. With the influences of biological processes, the highest $\delta^{13}C_{DIC}$ values are found in fall observations. The lowest DIC concentrations observed in fall are due mostly to the freshwater input which dilutes the DIC concentrations in the surface water. The mean values of DIC concentration and $\delta^{13}C_{DIC}$ in the surface water in the fall and spring are 2034±33 and 1987±52 μmol/kg, 1.3 ± 0.3 and 1.0 ± 0.2, respectively. The spring surface DIC concentration is higher than the fall values ($p<0.05$) due to the domination of respiration process while the $\delta^{13}C_{DIC}$ values prone to show the opposite results. Overall, the relationship between DIC and $\delta^{13}C_{DIC}$ is negative in both seasons, with the exception of the observations from NSC, which was discussed in section 3.2.

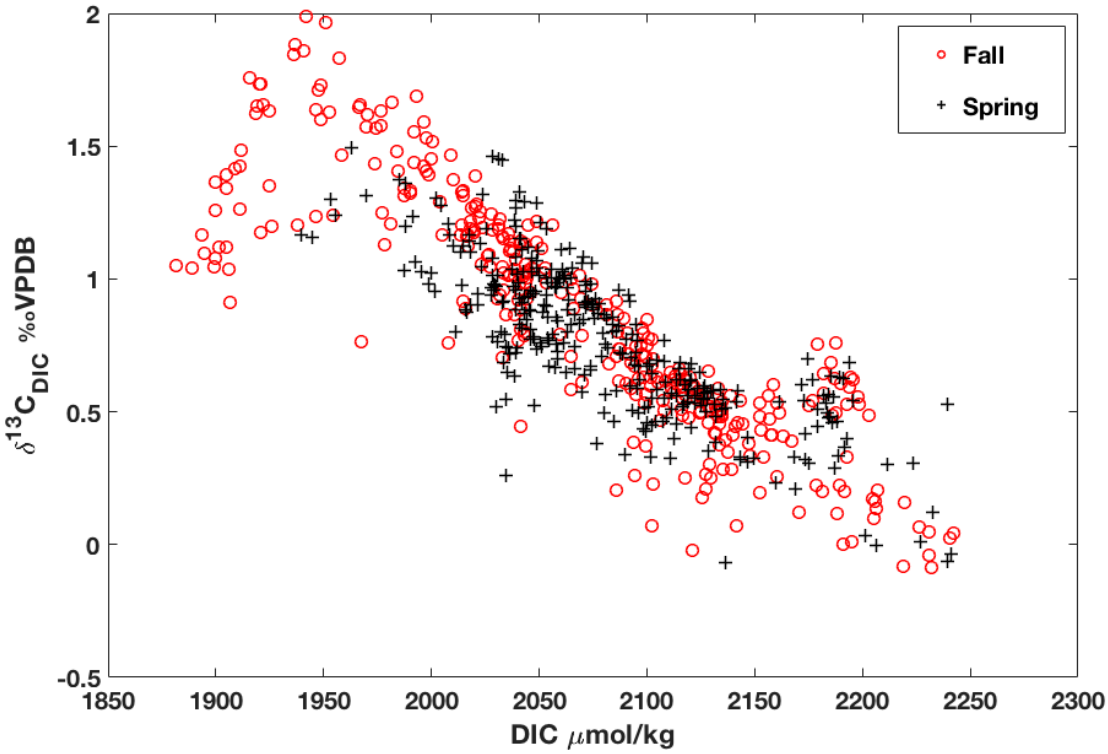

Fig. 11. $\delta^{13}C_{DIC}$ vs. DIC in the spring and fall of 2014. The red "o" sign represents samples observed in fall, and black "+" represents samples observed in spring.

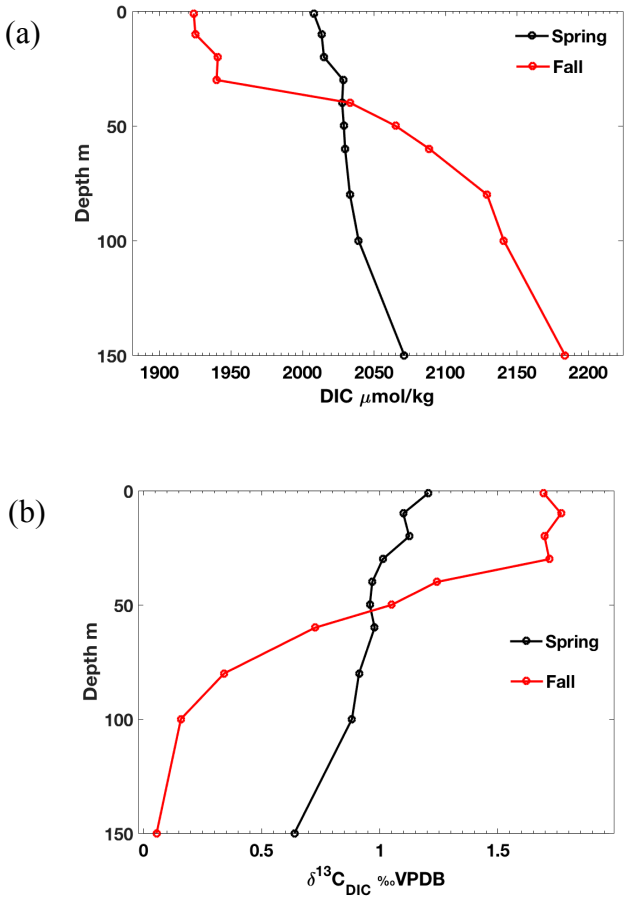

Fig. 12. Depth profiles of DIC (a) and $\delta^{13}C_{DIC}$ (b) for Halifax Line station 2 (HL2). The red and black color indicates data in the fall and spring, respectively. The profile is similar to the observations examined earlier in 2014, as reported by Lemay et al. (2018).

3.4 Governing Processes

In coastal regions, DIC concentrations and $\delta^{13}C_{DIC}$ values are influenced by biological processes (photosynthesis and respiration), freshwater input, calcium carbonate dissolution and formation, and air-sea exchange (e.g., Wong & Sackett, 1978; Winde et al., 2014a; Eide et al., 2017b). In order to examine the importance of these factors on the Scotian Shelf water, we followed the same approach described by Winde et al. (2014a)

and created a plot of $\delta^{13}C_{DIC}$ vs. DIC for data collected in the fall of 2014 to estimate the slopes for their governing processes (Fig. 15).

The invasion and outgassing of CO_2 can affect the $\delta^{13}C_{DIC}$ values in the surface water. The atmospheric CO_2 is isotopically light, during the invasion of CO_2 from the atmosphere to the ocean, DIC concentration in the surface water tends to increase while the $\delta^{13}C_{DIC}$ value decreases. Conversely, DIC concentration decreases while the $\delta^{13}C_{DIC}$ value increases during outgassing, as the light carbon is favored during this process. According to Lynch-Stieglitz et al. (1995), an addition of 1 μmol/kg carbon from the atmosphere into the North Atlantic would result in a decrease of 0.005‰ in $\delta^{13}C_{DIC}$ values in the surface water. The slope for the effect of air-sea exchange processes would present in a magnitude of -0.005‰ (Fig. 15). In the case of $CaCO_3$ dissolution and formation, since the fractionation factor of $CaCO_3$ formation is small (less than 2 ‰; Michaelis et al., 1985) and the dissolution process does not fractionate, we assume that these two processes only affect the DIC concentrations, resulting in a slope of 0 shown in the plot of $\delta^{13}C_{DIC}$ vs. DIC (Fig. 15). Additionally, as discussed in section 3.3, the $CaCO_3$ effect was deemed insignificant in the Scotian Shelf waters.

The $\delta^{13}C_{DIC}$ values in the Scotian Shelf surface waters in the fall ranged from 0.6 ‰ VPDB to 2.0 ‰ VPDB. The positive relationship between DIC and $\delta^{13}C_{DIC}$ shown in the surface water of CSL and LL (red arrow in Fig. 9) indicates a significant influence of river water input from the Gulf of St. Lawrence. Due to the dissolution of biogenic carbon in the soils, rivers and groundwater are usually depleted in $\delta^{13}C_{DIC}$ values (-25‰VPDB) (Spiker, 1980). Hélie et al. (2001) estimated the $\delta^{13}C_{DIC}$ values during the May of 1998 to April of 1999 in St. Lawrence River, yielding $\delta^{13}C_{DIC}$ values with a range of -14.2 ‰ to

0.9 ‰. Negative $\delta^{13}C_{DIC}$ values in the St. Lawrence River were also reflected in our observations. Previous studies have used the relationship between $\delta^{13}C_{DIC}$ and salinity to evaluate the salinity-dependent changes in $\delta^{13}C_{DIC}$ values and to estimate the end-members at different salinities (e.g., Spiker, 1980; Fry, 2002). Our freshwater samples ($S \leq 30$, where mostly influenced by river water input) yielded a zero-salinity end member of -9.5 (±3.8) ‰VPDB (Fig. 13), which is in agreement with the above literature value.

A linear least squares regression of DIC as a function of salinity is a commonly used method to evaluate the salinity dependent changes in DIC and examine the mixing of different water masses (e.g., Thomas & Schneider, 1999; Osterroht & Thomas, 2000; Fry, 2002). The DIC concentration at zero salinity is calculated from the observations on the central Scotian Shelf, which yields a $DIC_{S=0}$ concentration of 804 ±89 µmol/kg (TA=730±21 µmol/kg) (Fig. 14). Selecting the stations at the central shelf, instead of including the offshore stations, makes our results comparable to Shadwick's observations ($DIC_{S=0}$ = 633±91) from samples taken at the same stations in 2007 (Fig. 14). This TA value is also consistent with Shadwick et. al's observation in 2011 (TA=805 ±12 µmol/kg) and Bay of Fundy (TA=709±13 µmol/kg) (Horwitz et al., 2019). A two-point mixing line with a slope of 0.01 ‰VPDB per µmol/kg DIC is calculated by using the estimated values (DIC=804 µmol/kg; $\delta^{13}C_{DIC}$ = -9.5 ‰VPDB) of a river endmember (St. Lawrence River) along with the average values (average surface DIC=1987±52 µmol/kg; average surface $\delta^{13}C_{DIC}$=1.3±0.3 ‰VPDB) calculated from the Scotian Shelf water in 2014 (Fig. 15). This slope of 0.01 ‰VPDB per µmol/kg DIC is considered to represent the river water influences on the DIC vs $\delta^{13}C_{DIC}$ distribution on the Scotian Shelf (Fig. 15).

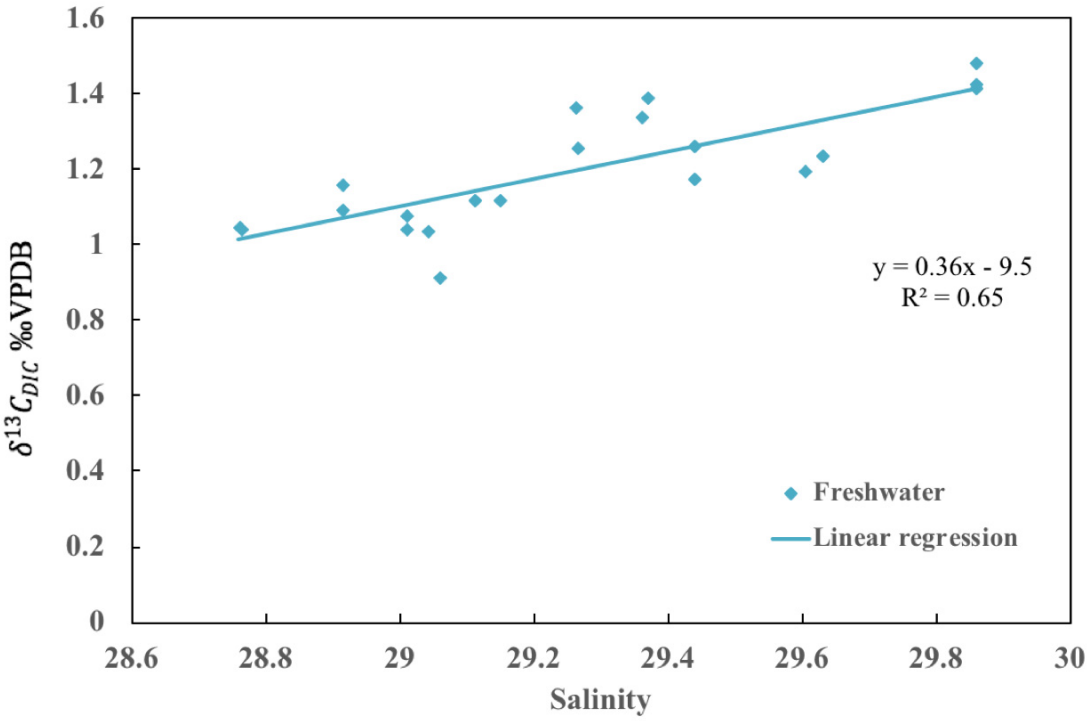

Fig. 13. The relationship between $\delta^{13}C_{DIC}$ and salinity in the freshwater observations, where $\delta^{13}C_{DIC}$ = 0.36 (±0.13) × Sal - 9.5 (±3.8), R^2=0.65.

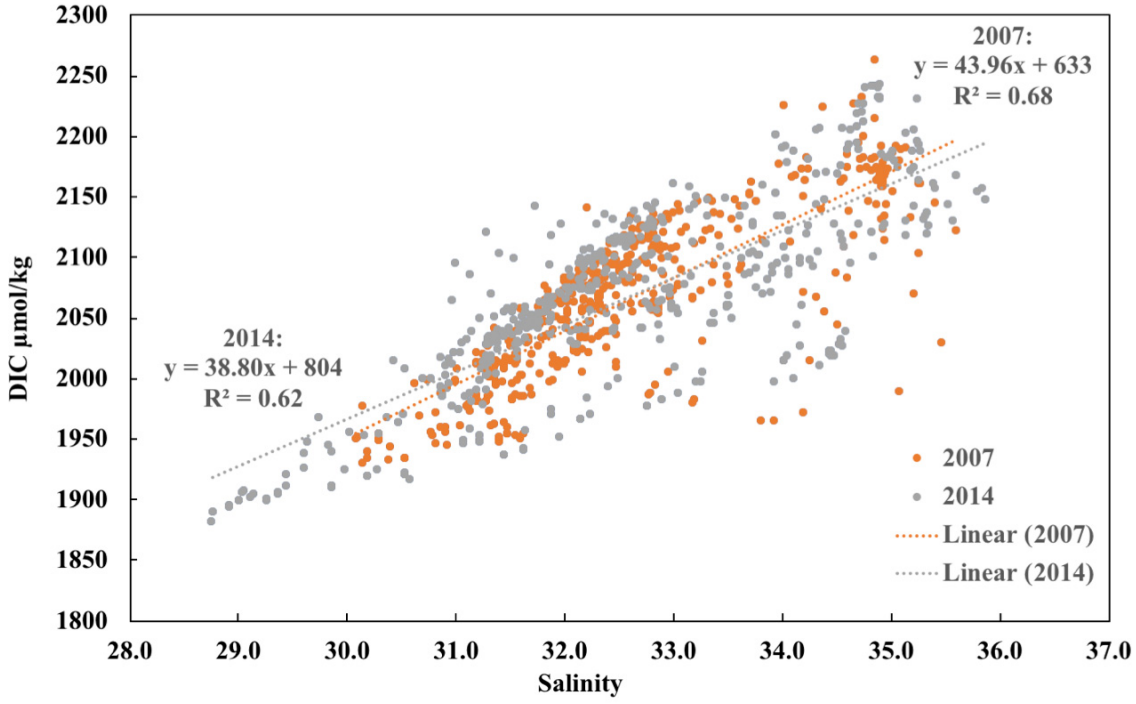

Fig. 14. The relationship between DIC and salinity in our observations (spring and fall 2014) as well as Shadwick's observations (the samples were taken in the spring and fall of 2007). Note that all the observations we presented in this figure are the samples taken from the central Scotian Shelf, which only includes stations in BBL1-6, HL1-7, LL1-7, and CSL1-6. The gray and orange dash lines are obtained from linear least-squares regression of our observations (from 2014) and Shadwick's observations (from 2007), which yield results of DIC=38.8 (±2.7) × Sal + 804 (±89) (R^2=0.62), and DIC=43.96 (±2.8) × Sal + 633 (±91) (R^2=0.68), respectively.

The other end-member of this region is the Labrador Shelf water (LShW), which is influenced by water masses of Arctic origin, entering the Scotian Shelf via the Labrador and Newfoundland Shelves (Urrego-Blanco & Sheng, 2012; Thomas et al., 2012). Due to the ice formation on the Gulf of St Lawrence in the winter and early spring, the NSC is dominated by, instead of the St Lawrence Estuary water, but the LShW, which is influenced by the relatively freshwater of the Arctic origin. Therefore, we used the observations from the surface water in the spring 2014 and obtained linear least-squares regression lines between $\delta^{13}C_{DIC}$ and salinity (where $\delta^{13}C_{DIC}$ = -0.09 ±0.04 × Sal + 4.10±1.33, R^2=0.3), as well as between DIC and salinity (where DIC= 16.83 ±3.27 ×Sal + 1495 ±108, R^2=0.64) to estimate the $\delta^{13}C_{DIC}$ value and DIC concentration for this end-member. The freshwater from the Arctic region was mainly from the snow and glacier meltwater from areas without soil cover or vegetation and bacterial decay of organic matter, therefore the DIC of which equilibrates with the atmosphere and presents high values of $\delta^{13}C_{DIC}$, with a mean value reported as 1.13 ± 0.2 ‰VPDB (Mackensen et al., 2013). Our result yielded a $DIC_{S=32}$ (DIC concentration at salinity equals to 32) and a $\delta^{13}C_{DICS=32}$ ($\delta^{13}C_{DIC}$ value at salinity equals to 32) value of 2034 ± 108 μmol/kg and 1.14 ± 0.04 ‰VPDB, respectively. This estimated $\delta^{13}C_{DIC}$ value of the Arctic water end-member

is consistent with the value reported by Mackensen et al. (2013). The slope for this end-member influences can be again calculated by the two-point mixing method described above and yielded a result of -0.0028 ‰VPDB per μmol/kg DIC (Fig. 15).

Biological processes have significant influence on the carbon cycling in the Scotian Shelf water through photosynthesis and respiration, especially during the warm seasons. In order to further understand this biological governing process, we use two methods for cross-validation and to interpret the relationship between $\delta^{13}C_{DIC}$ and DIC obtained from the fall of 2014.

According to Broecker and Maier-Reimer (1992), when assuming the distribution of $\delta^{13}C_{DIC}$ in seawater is solely due to biological processes, then $\delta^{13}C_{DIC}$ should be tightly related to the dissolved phosphate concentration. The relationship between these two variables would yield a slope of *k*:

$$k = \frac{f}{DIC_{avg}} * [\frac{C}{P}]_{org} \quad (3.1)$$

where *f* is the biological fractionation factor, DIC_{avg} is the average DIC concentration, and $[\frac{C}{P}]_{org}$ is the carbon to phosphate ratio in organic matters. Given the above equation, considering only biological processes, the slope of $\delta^{13}C_{DIC}$ against DIC can be calculated by $k/[\frac{C}{P}]_{org}$ (or f/DIC_{avg}). Based on this method, the slope of the biological processes influences on the Scotian Shelf is calculated by dividing the biological fractionation factor in marine primary producer over the average DIC concentration in the Scotian Shelf waters. The average biological fractionation factor for marine plankton (f) is -25 ‰ (Sackett et al., 1965) and the average surface DIC on the Scotian Shelf is 1987 ±52 μmol/kg, together

yielding a slope of -0.012 ‰VPDB per µmol/kg DIC, which represents the theoretical biological effect on the covariation between $\delta^{13}C_{DIC}$ and DIC (Fig. 15).

The linear least-squares regression of the $\delta^{13}C_{DIC}$ vs. DIC distribution represents the best-fit line 1 and yields a slope of -0.0046 ±0.0003 ‰VPDB per µmol/kg DIC (R^2=0.75). Comparing the best-fit line 1 with other slopes of different controlling processes, the biological processes with a slope of -0.012 ‰VPDB per µmol/kg DIC has a strong influence on controlling the negativity of the best-fit line 1, while other processes tend to bias the slope in opposing direction. This indicates the importance of photosynthesis and respiration in governing the covariation on the Scotian Shelf. However, this analysis cannot eliminate the effects of air-sea exchange and river water or Arctic water input on biasing the slope of the best-fit line 1. To further understand the biological impact and other processes on the Scotian Shelf waters and to cross-validate the above method, DIC_{bio} is introduced, which separates the biologically derived DIC from other contributions.

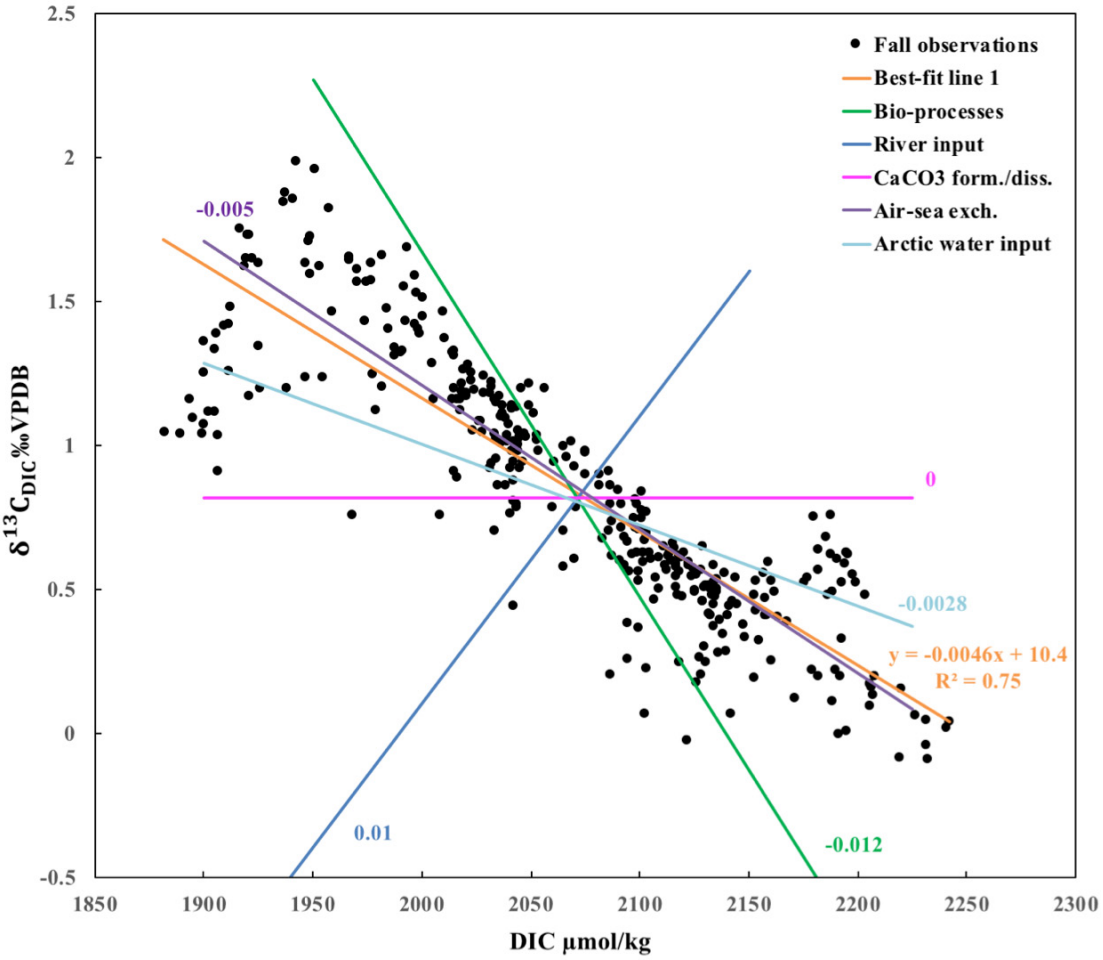

Fig. 15. The relationship between $\delta^{13}C_{DIC}$ and DIC in Scotian Shelf waters (above 500 m) in the fall of 2014. The green, blue, pink, aqua, and purple straight lines and numbers indicate the estimated slopes for biological processes, river input, $CaCO_3$ formation or dissolution, and air-sea exchange effects, and Arctic water input, respectively. The orange line is obtained from the linear least-squares regression of the data, where $\delta^{13}C_{DIC}$ = -0.0050 (±0.0003) × DIC + 10.4 (±0.6), R^2=0.75.

The DIC_{bio} term, as discussed in section 2.3, assumes that the water is equilibrated with the atmosphere prior to any biological influence. Based on this assumption, DIC_{bio} values are obtained by taking the difference of the DIC concentrations under air-sea equilibrium from the observed DIC concentrations. Since the adjustment of the isotopic equilibrium of $\delta^{13}C_{DIC}$ between air and sea is much slower (about 10 times) than the chemical equilibrium of CO_2 (Tans, 1980; Lynch-Stieglitz et al., 1995), and the residence time of water in the

Scotian Shelf is relatively short (couple of days to 30 days; Smith et al, 2003; Shan, 2016) compared to the open ocean, the influence of air-sea exchange process on the DIC_{bio}-$\delta^{13}C_{DIC}$ relationship in the Scotian Shelf waters is deemed insignificant. The effects of river and Arctic water input are indicated as vertical slopes in Fig. 16, suggesting that these freshwater inputs would only change $\delta^{13}C_{DIC}$ values since the DIC_{bio} terms normalize for any salinity-dependent changes in DIC.

The slope of best-fit line 2 (-0.011 ‰VPDB per μmol/kg DIC) compares well with the slope of biological processes (-0.012 ‰VPDB per μmol/kg DIC), which again suggests the importance of biological processes on the covariation between DIC and $\delta^{13}C_{DIC}$ (Fig. 16). For quantifying the relationship between DIC_{bio} and $\delta^{13}C_{DIC}$, the slope of -0.011 (‰ VPDB per μmol/kg DIC) indicates that a biological change in DIC concentrations by 1 μmol/kg relates to a change of 0.011 ‰VPDB in the $\delta^{13}C_{DIC}$ value. With a slope of -0.011 (‰VPDB per μmol/kg DIC), we were also able to calculate a biological fractionation factor using equation 3.1, which yielded a result of -22‰ (‰VPDB per μmol/kg DIC). This calculated biological fractionation factor is comparable to the literature values (-18‰ ~ -30‰, Sackett et al., 1965; -14‰ ~ -31‰, Descolas-Gros & Fontugne, 1990), and provides a baseline of estimation for further studies.

These two methods used above are able to cross-validate each other, and they both suggest that the biological processes are an essential governing process on $\delta^{13}C_{DIC}$ and DIC distribution in the fall in the Scotian Shelf waters. As proposed by others (Burt et al., 2013; Winde et al., 2014a, b; Clargo et al, 2015; Burt et al. 2016), using DIC_{bio} also helps unravel the various processes shown in Fig. 15. This further provides the estimates of quantification on the relationship between DIC and its isotopic composition as well as the

biological fractionation factor on the Scotian Shelf. To further quantify the biological component between the spring and fall in 2014, the net community production (NCP) in the study region was investigated.

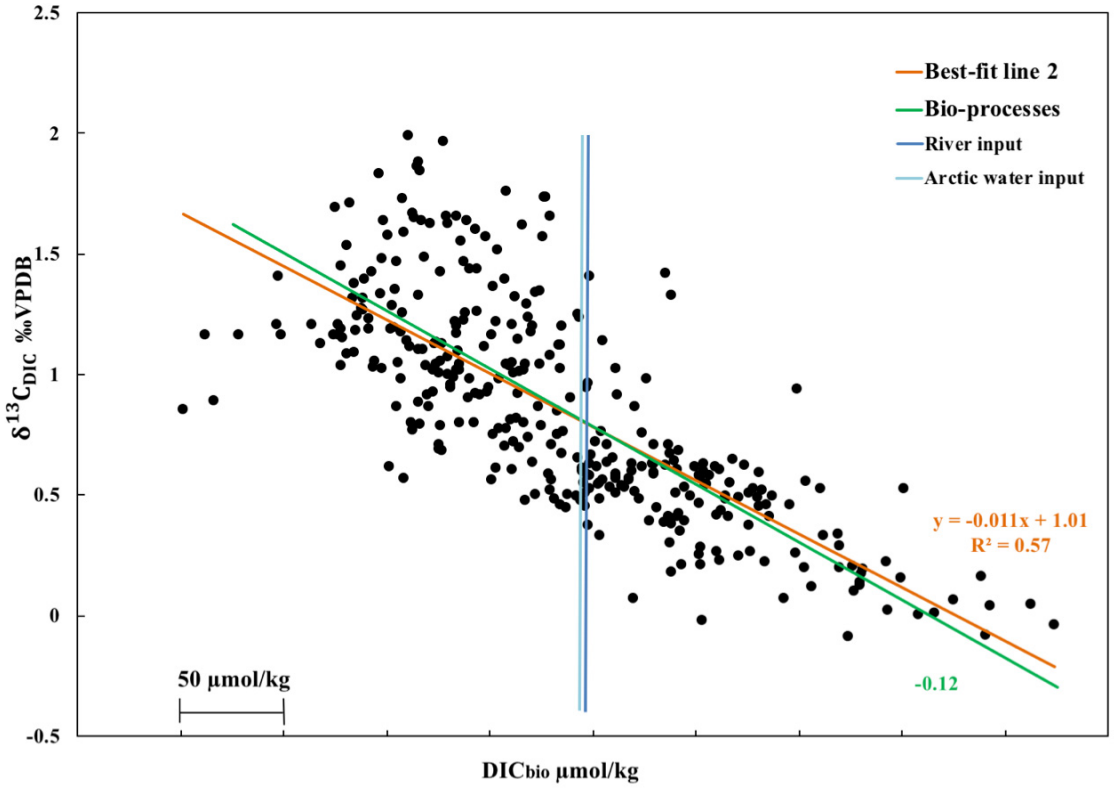

Fig. 16. The relationship between $\delta^{13}C_{DIC}$ and DIC_{bio} in the Scotian Shelf waters (above 500 m) in the fall of 2014. The linear least square regression indicated by the orange colored line is the best-fit line of the data, where $\delta^{13}C_{DIC}$ = -0.011 (±0.001) × DIC_{bio} + 1.007 (±0.034), R^2=0.57. The blue and aqua lines represent the river and Arctic water input. DIC_{bio} is a relative variable, and each tick mark shows a DIC_{bio} change of 50 µmol/kg.

3.5 Net Community Production

Net community production (NCP) is the difference between autotrophic production of organic carbon (NPP) and heterotrophic production of CO_2 (R) at the space and time scales of the measurement (Serret et al., 2009):

$$NCP = NPP - R \tag{3.2}$$

Using the equation above, the metabolic state of a system can be defined. A positive NCP indicates an autotrophic system, where the production is greater than the respiration, leading to a loss of DIC in the water. Conversely, a negative NCP indicates a heterotrophic system and thus a gain in DIC in the water.

We use the following equation to quantify the cumulative NCP in the mixed layer of Scotian Shelf waters during April and October:

$$Cumulative\ NCP = \int_{Z=0}^{Z=40} \frac{n\delta^{13}C_{DICdiff}}{-0.012}\, dz \tag{3.3}$$

$$n\delta^{13}C_{DICdiff} = \delta^{13}C_{DICdiff(S-F)} - Sal_{diff(S-F)} \times 0.36 \tag{3.3a}$$

where $n\delta^{13}C_{DICdiff}$ is the difference of $\delta^{13}C_{DIC}$ between spring and fall after taking out the changes in $\delta^{13}C_{DIC}$ due to freshwater influence (equation 3.3a). It is calculated by taking the difference between the seasonal changes in $\delta^{13}C_{DIC}$ value ($\delta^{13}C_{DICdiff(S\text{-}F)}$) and the difference in $\delta^{13}C_{DIC}$ affected by the salinity changes due to freshwater input ($Sal_{diff(S\text{-}F)}\times 0.36$). The 0.36 is the slope of the linear regression line between $\delta^{13}C_{DIC}$ and salinity in the freshwater (Fig. 13, section 3.4). The -0.012 (‰VPDB per µmol/kg DIC) is the slope of theoretical biological effect mentioned in section 3.4. The climatological mixed layer depth on the Scotian Shelf is 40 m (Shadwick & Thomas, 2014), thus we integrated over the upper 40 m waters to account for the vertical mixing and ruled out the entrainment from deeper water. Furthermore, for better comparison with Shadwick and Thomas's (2014) results from their samples taken in 2007, choosing the same integrated depth of the mixed layer is beneficial. The uncertainty associated with NCP estimations was calculated using Monte Carlo simulations. The inputs for the simulation were randomly generated from normal distributions and 100,000 points were chosen randomly for each of the model variables using MATLAB (Mathworks, Inc.).

As discussed in section 3.4, the effect on $\delta^{13}C_{DIC}$ by air-sea exchange and $CaCO_3$ dissolution and formation can be neglected when quantifying the seasonal changes in $\delta^{13}C_{DIC}$ values. By taking out the salinity effect on $\delta^{13}C_{DIC}$ from the difference of $\delta^{13}C_{DIC}$ values between the spring and fall, we assume that the value of $n\delta^{13}C_{DICdiff}$ is only controlled by biological processes. Dividing this value by the biological processes factor (-0.012) and integrating over 40 m, the seasonal changes in DIC over six months, due solely to biological effects, can be calculated.

The estimated cumulative NCP (in molC m^{-2} per 6 months) and monthly NCP (molC m^{-2} $month^{-1}$) in the mixed layer at all stations along the four transects are provided in Table 1. Along the Browns Bank Line, the cumulative NCP values in the mixed layer at all stations are mostly positive, with a mean value of 0.31 ± 1.56 molC m^{-2} per 6 months. This is in agreement with the mean cumulative NCP value (over 6 months) along BBL in 2007 calculated by Shadwick and Thomas (2014), of 0.6 molC m^{-2} per 6 months. The highest values were found in the nearshore stations (BBL 1 and 2) along BBL (Table 1). In the Halifax Line, nearshore stations presented comparably higher values of NCP, with the maximum values found at HL 3 and HL 5. The average cumulative NCP along the Halifax Line was 0.25 ± 1.73 molC m^{-2} per 6 months, and it was higher than the value calculated by Shadwick and Thomas from their 2007 data by 0.15 molC m^{-2} per 6 months ($p<0.05$) (2014). Along the Louisburg Line, the cumulative NCP are mostly positive except at the last two offshore stations, the average cumulative NCP along this transect was 0.68 ± 2.34 molC m^{-2} per 6 months. Negative cumulative NCP calculated by Shadwick and Thomas was only found in the CSL, while negative values in our calculations were found in all transects (2014). The mean cumulative NCP along the Cabot Strait Line was 0.24 ± 0.98

molC m^{-2}, with negative values found at stations CSL 1, 4 and 5. The highest cumulative NCP value was found in LL, the second highest value was found in BBL, and CSL exhibits the lowest value. This trend is in agreement with the trend found in Shadwick and Thomas's calculations.

Table 1. The estimated cumulative NCP (NCP cumulative) over six months and monthly NCP (NCP monthly) in the climatological mixed layer of Scotian Shelf waters. The uncertainties associated with the values are indicated in the brackets, accordingly. Note the unit for cumulative NCP is molC m^{-2} per 6 months and the unit for NCP monthly is molC m^{-2} $month^{-1}$.

Station	NCP cumulative	NCP monthly
Browns Bank Line		
BBL1	2.36(0.03)	0.39(0.01)
BBL2	1.75(0.30)	0.29(0.05)
BBL3	-1.50(0.76)	-0.25(0.13)
BBL4	-2.29(1.03)	-0.38(0.17)
BBL5	0.83(0.18)	0.14(0.03)
BBL6	0.15(0.32)	0.03(0.05)
BBL7	0.89(0.29)	0.15(0.05)
BBL mean	0.31(1.56)	0.05(0.26)
Halifax Line		
HL1	1.29(0.20)	0.21(0.03)
HL2	-2.08(0.46)	-0.35(0.08)
HL3	2.16(0.15)	0.36(0.03)
HL4	3.45(0.29)	0.57(0.05)
HL5	2.52(0.08)	0.42(0.01)
HL6	0.71(0.09)	0.12(0.01)
HL7	-1.90(0.76)	-0.32(0.13)
HL8	-1.21(0.65)	-0.20(0.11)
HL9	-1.01(0.68)	-0.17(0.11)
HL10	-0.75(0.74)	-0.12(0.12)
HL11	-0.62(0.56)	-0.10(0.09)
HL12	0.46(0.01)	0.08(0.00)
HL mean	0.25(1.73)	0.04(0.29)
Louisburg Line		
LL1	2.06(0.52)	0.34(0.09)

Station	NCP cumulative	NCP monthly
LL3	1.36(0.37)	0.23(0.06)
LL2	2.15(0.40)	0.36(0.07)
LL4	2.69(0.31)	0.45(0.05)
LL5	2.85(0.63)	0.48(0.10)
LL6	1.55(0.27)	0.26(0.05)
LL7	0.05(0.26)	0.01(0.04)
LL8	-2.05(0.96)	-0.34(0.16)
LL9	-4.54(1.27)	-0.76(0.21)
LL mean	0.68(2.34)	0.11(0.39)
Cabot Strait Line		
CSL1	-0.18(0.23)	-0.03(0.04)
CSL2	1.62(0.37)	0.27(0.06)
CSL3	1.26(0.44)	0.21(0.07)
CSL4	-1.45(0.38)	-0.24(0.06)
CSL5	-0.86(0.16)	-0.14(0.03)
CSL6	1.08(0.11)	0.18(0.02)
CSL mean	0.24(0.98)	0.04(0.16)
Total mean	0.38 (1.81)	0. 06(0.30)

The monthly NCP is calculated by dividing the cumulative NCP over 6 months and the values for each station along the four transects are illustrated in Fig. 17. The overall patterns show that the mixed layer on the shelf tends to present as an autotrophic system while the mixed layer offshore shows a heterotrophic system. The mechanism or reasoning behind is not discussed in this research and would need to be investigated future research for further reference.

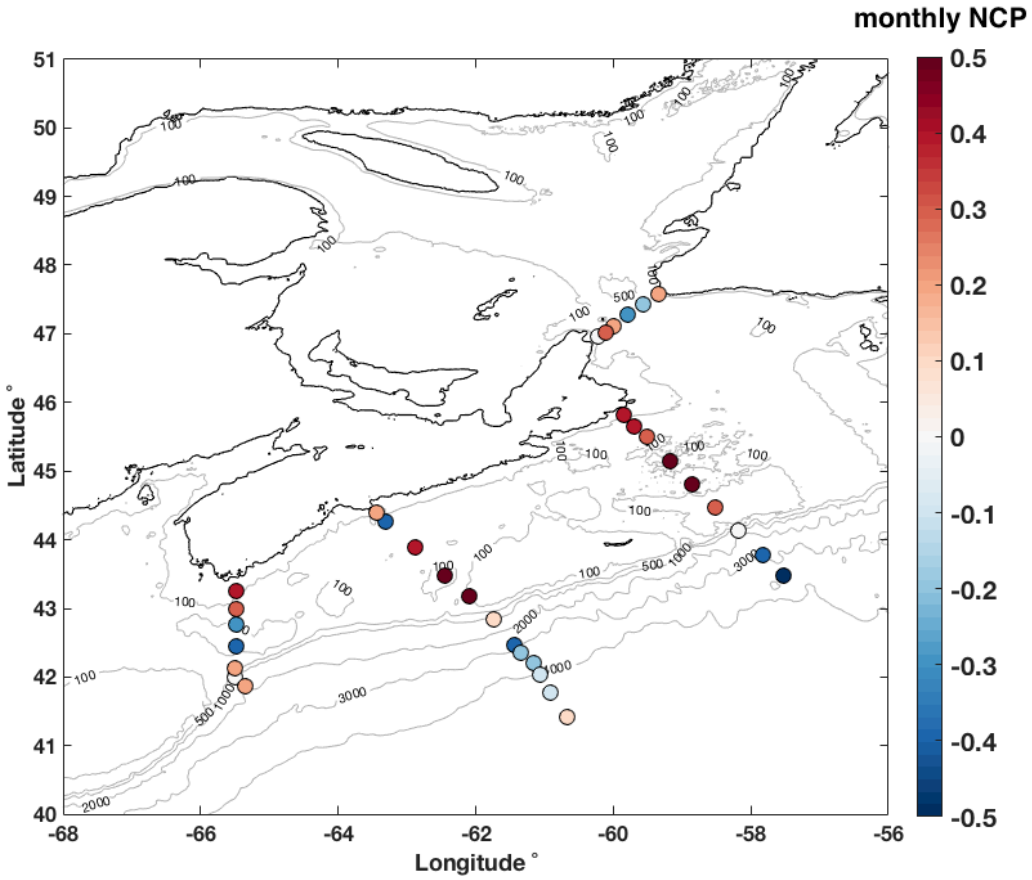

Fig. 17. Monthly NCP ($molCm^{-2}month^{-1}$) at each station along the four transects. Positive NCP indicates an autotrophic system while the negative NCP indicates a heterotrophic system.

Our estimates for monthly NCP ranged from -0.76 to 0.57 molC m^{-2} $month^{-1}$, which is slightly lower than the estimates calculated by Shadwick and Thomas (2014) for the observations in 2007 (0.1 to 0.8 molC m^{-2} $month^{-1}$). The difference between these estimates could be due to variations in NCP in different years. For example, Shadwick et al. investigated the distribution of chlorophyll-*a* (chl-*a*) through satellite data on the Scotian Shelf from the year 1999 to 2008 (2010, their Figs. 5a & 10). The estimated partial pressure of CO_2 based on chl-*a* on the shelf vary substantially between years due to the temporal variation of chl-*a* in the region. Although the NCP estimates were not specified

in Shadwick et al.'s study, the variations of NCP in different years due to the same reason can be surmised.

Different methods used to calculate the estimated NCP could also contribute to the different results. To compute the NCP from the observed data in 2007, Shadwick and Thomas (2014) used a simple salinity normalization method to calculate the seasonal change in salinity normalized (S=35) DIC, which eliminated freshwater influence on DIC when computing NCP in the region. The contributions from the air-sea exchange, entrainment from the deep water, and the biological processes have all been accounted for in the computed seasonal changes in normalized DIC. In our method, we were able to separate the changes in DIC solely controlled by biological processes from other factors that contribute to the changes in DIC. By using this method, it could result in different NCP values compared to using Shadwick and Thomas' method (2014). To test this, we also computed our observations (from 2014) following the same procedure as Shadwick and Thomas (2014); the resulting monthly NCP ranged from 0.1 to 0.9 molC m^{-2} $month^{-1}$, which was higher than our original NCP estimates (-0.76 to 0.57 molC m^{-2} $month^{-1}$) and also agreed well with Shadwick and Thomas' result (0.1 ~ 0.8 molC m^{-2} $month^{-1}$).

NCP can be computed based on DIC, nitrate, or biomass through different methods and techniques. Shadwick and Thomas (2014) compared the estimated NCP on the Scotian Shelf based on DIC and nitrate. They concluded that the estimated nitrate-based NCP_N was significantly lower than the carbon-based estimates (NCP_C), due to ongoing biological production in nitrate-depleted waters. Bozec et al. (2006) estimated NCP in the North Sea based on DIC and nitrate, they also concluded that the NCP based on nitrate would lead to an underestimation of NCP compared to NCP_C, since the phytoplankton abundant in the North Sea permits the consumption of DIC in nutrient depleted waters. In 2010, Shadwick

et al. also computed NCP_B based on biomass through (chl-*a* based) satellite estimates, which resulted in an underestimation of NCP compare to NCP_C. The substantial loss of chl-*a* from the surface layer due to sinking and grazing leads to an underestimated NCP_B, which emphasizes the advantage of the DIC based method of computing NCP (Shadwick et al., 2010; Shadwick et al., 2011). In this study, NCP is estimated based on DIC, particularly, $\delta^{13}C_{DIC}$, which separates the biological effect from other factors so that the seasonal changes in DIC solely due to biological processes are enabled to be calculated.

The NCP values estimated by Ostle et al. in the region between 14 °N and 50 °N in North Atlantic range from 0.17 to 0.59 molC m^{-2} $month^{-1}$, with the region lies between 14 °N and 30 °N present the lower value while the region lies between 40 °N and 50 °N, close to the eastern side of North Atlantic, shows the highest value (2015). The NCP estimate in North Sea could be higher than the NCP in North Atlantic, with a value on the order of 0.67 molC m^{-2} $month^{-1}$ (assuming the productive seasons last for 6 months) (Thomas et al., 2005). In the Arctic Ocean basin, the NCP ranges from 0.038 molC m^{-2} $month^{-1}$ to 0.063 molC m^{-2} $month^{-1}$, and is deemed perennially oligotrophic (Bates, Best & Hansell, 2005; Anderson et al., 2003). Comparing our results with the literature values mentioned above, our estimated value of monthly NCP (0.06±0.3 molC m^{-2} $month^{-1}$) seems small, and this is because that the mixed layer of Scotian Shelf water in 2014 exhibits both autotrophic and heterotrophic systems. The uncertainty associated with our NCP estimate is mainly due to changes in temperature, with a value of 0.2 molC m^{-2} $ºC^{-1}$ (Takahashi et al.,1993).

CHAPTER 4. CONCLUSION

This study investigated carbonate system parameters including TA, DIC, and $\delta^{13}C_{DIC}$ in the Scotian Shelf waters during April and October of 2014. The objective of this study was to assess the current inorganic carbon cycling situation on the Scotian Shelf and to set up a baseline for future studies. With respect to our hypothesis, we accept the first and second hypothesis and reject the third hypothesis. The concentration of DIC is higher in the mixed layer of Scotian Shelf waters in spring compared to the fall condition, while the $\delta^{13}C_{DIC}$ values gives the opposite result. The quantitative analysis of the relationship between DIC and $\delta^{13}C_{DIC}$, as well as the use of DIC_{bio}, successfully unravel the various governing processes on the inorganic carbon cycling in the study region. This suggests that biological processes and freshwater input are playing significant roles, therefore confirming our hypothesis. The surface layer of the Scotian Shelf is characterized as both autotrophic and heterotrophic, and its monthly NCP in the mixed layer of Scotian Shelf water is ranges from -0.76 to 0.57 molC m^{-2} $month^{-1}$ and the mean value is reported as 0.06 molC m^{-2} $month^{-1}$, hence we reject our third hypothesis. The estimated NCP is calculated based on DIC converted from $\delta^{13}C_{DIC}$ values, which is a potentially improved method compared to the method used by Shadwick and Thomas (2014). Based on this study, we put confidence in using the isotope approach on the NCP assessment; however, data sets vary in coverage, space and time hampers the detailed comparison of methods between studies. Hence, using consistent data sets that can apply to all methods would be beneficial in future studies.

Bibliography

Anderson, L. G., Jones, E., P., & Swift, J. H. (2003). Export production in the central Arctic Ocean evaluated from phosphate deficits. *Journal of Geophysical Research: Oceans, 108*(C6).

Archer, D., Kheshgi, H., & Maier-Reimer, E. (1997). Multiple timescales for neutralization of fossil fuel CO_2. *Geophysical Research Letters, 24*(4), 405-408.

Atlantic Coastal Zone Information Steering Committee. (2016). State of the Scotian Shelf. Retrieved from http://coinatlantic.ca/index.php/state-of-the-scotian-shef

Bates, N. R., Best, M. H., & Hansell, D. A. (2005). Spatio-temporal distribution of dissolved inorganic carbon and net community production in the Chukchi and Beaufort Seas. *Deep Sea Research Part II: Topical Studies in Oceanography*, *52*(24-26), 3303-3323.

Bindoff, N. L., Willebrand, J., Artale, V., Cazenave, A., Gregory, J. M., Gulev, S., ... & Shum, C. K. (2007). Observations: oceanic climate change and sea level.

Böttcher, M. E. (1999). The stable isotopic geochemistry of the sulfur and carbon cycles in a modern karst environment. *Isotopes in environmental and health studies*, *35*(1-2), 39-61.

Broecker W. S., & Maier-Reimer, E. (1992). The influence of air and sea exchange on the carbon isotope distribution in the sea. *Global Biogeochemical Cycles*, *6*(3), 315-320.

Brewer, P. G. & Goldman J. C. (1976). Alkalinity changes generated by phytoplankton growth, *Limnology and Oceanography.*, *21*, 108-117.

Burt, W., Thomas, H., & Auclair, J. P. (2013). Short-lived radium isotopes on the Scotian Shelf: Unique distribution and tracers of cross-shelf CO_2 and nutrient transport. *Marine Chemistry*, *156*, 120-129,

Burt, W. J., Thomas, H., Hagens, M., Patsch, J., Clargo, N.M, Salt, L.A., Winde, V., & Böttcher, M.E. (2016). Carbon sources in the North Sea evaluated by means of radium and stable carbon isotope tracers. *Limnology and Oceanography. 61*, 666-683.

Chapman, D. C., & Beardsley, R. C. (1989). On the origin of shelf water in the Middle Atlantic Bight. *Journal of Physical Oceanography*, *19*(3), 384-391.

Clargo, N. M., Salt, L. A., Thomas, H., & de Baar, H. J. W. (2015). Rapid increase of observed DIC and pCO_2 in the surface waters of the North Sea in the 2001-2011

decade ascribed to climate change superimposed by biological processes. *Marine Chemistry*, *177*, 566-581. Retrieved from https://doi.org/10.1016/j.marchem. 2015.08.010

Craig, H. (1953). The geochemistry of the stable carbon isotopes. *Geochimica et cosmochimica acta*, *3*(2-3), 53-92.

Craig, H. (1957). Isotopic standards for carbon and oxygen and correction factors for mass-spectrometric analysis of carbon dioxide. *Geochimica et cosmochimica acta*, *12*(1-2), 133-149.

Craig, S. E., Thomas, H., Jones, C. T., Li, W. K. W., Greenan, B. J. W., Shadwick, E. H., & Burt, W. J. (2014). The effect of seasonality in phytoplankton community composition on CO_2 uptake on the Scotian Shelf, *Journal of Marine System*, *147*, 52–60.

Deines, P., Langmuir, D., & Harmon, R. S. (1974). Stable carbon isotope ratios and the existence of a gas phase in the evolution of carbonate ground waters. *Geochimica et Cosmochimica Acta*, *38*(7), 1147-1164.

Descolas-Gros, C., & Fontungne, M. (1990). Stable carbon isotope fractionation by marine phytoplankton during photosynthesis. *Plant, Cell & Environment*, *13*(3), 207-218.

Dickson, A. G., Sabine, C. L., & Christian, J. R. (2007). Guide to best practices for ocean CO2 measurements, *PICES Special Publications, 3*.

Doney, S. C., Fabry, V. J., Feely, R. A., & Kleypas, J. A. (2009). Ocean acidification: the other CO_2 problem.

Dorsett, A., Cherrier, J., Martin, J. B., & Cable, J. E. (2011). Assessing hydrologic and biogeochemical controls on pore-water dissolved inorganic carbon cycling in a subterranean estuary: A ^{14}C and ^{13}C mass balance approach. *Marine Chemistry*, *127*(1-4), 76-89.

Eide, M., Olsen, A., Ninnemann, U., & Johannessen, T. (2017a). A global ocean climatology of preindustrial and modern ocean $\delta^{13}C_{DIC}$, *Global Biogeochemical Cycles, 31*, 515–534.

Eide, M., Olsen, A., Ninnemann, U. S., & Eldevik, T. (2017b). A global estimate of the full oceanic 13C Suess effect since the preindustrial. *Global Biogeochemical Cycles*, *31*(3), 492-514.

Emerson, S., Quay, P., Karl, D., Winn, C., Tupas, L., & Landry, M. (1997). Experimental determination of the organic carbon flux from open-ocean surface waters. *Nature*, *389*(6654), 951.

Fisheries and Oceans Canada. (2014a). *Scotian Shelf: An Atlas of Human Activities.* Retrieved from http://www.mar.dfompo.gc.ca/Maritimes/Oceans/OCMD/Atlas/Oil-Gas-Industry

Fisheries and Oceans Canada. (2014b). Regional Oceans Plan. Retrieved from http://waves-vagues.dfo-mpo.gc.ca/Library/365205.pdf

Fournier, R. O., Marra, J., Bohrer, R., & Det, M. V. (1977). Plankton dynamics and nutrient enrichment of the Scotian Shelf. *Journal of the Fisheries Board of Canada*, *34*(7), 1004-1018.

Fry, B. (2002). Conservative mixing of stable isotopes across estuarine salinity gradients: a conceptual framework for monitoring watershed influences on downstream fisheries production. *Estuaries*, *25*(2), 264-271.

Gatien, M. G. (1976). A study in the slope water region south of Halifax. *Journal of the Fisheries Board of Canada*, *33*(10), 2213-2217.

Gattuso, J. P., Frankignoulle, M., & Wollast, R. (1998). Carbon and carbonate metabolism in coastal aquatic ecosystems. *Annual Review of Ecology and Systematics, 29*, 405–434.

Gearing, P., Plucker, F.E., Parker, P.L. (1977). Organic carbon stable isotope ratios of continental margin sediments. *Marine Chemistry, 5*, 251-266

Gilbert, D., Gobeil, C., Sundby, B., Mucci, A., & Tremblay, G.-H. (2005). A seventy-two-year record of diminishing deep-water oxygen levels in the St. Lawrence estuary: The northwest Atlantic connection. *Limnology and Oceanograph*, *50*, 1654–1666.

Gledhill, D. K., White, M. M., Salisbury, J., Thomas, H., Mlsna, I., Liebman, M., … Doney, S. C. (2015). Ocean and Coastal Acidification off New England and Nova Scotia. *Oceanography*, *28*(2), 182-197.

Gruber, N., Keeling, C. D., & Stocker, T. F. (1998). Carbon-13 constraints on the seasonal inorganic carbon budget at the BATS site in the northwestern Sargasso Sea. *Deep Sea Research Part I: Oceanographic Research Papers*, *45*(4-5), 673-717.

Gruber, N., Keeling, C. D., Bacastow, R. B., Guenther, P. R., Lueker, T. J., Wahlem, M., Meijer, H. A. J., … Stocker, T. F. (1999). Spatiotemporal patterns of carbon-13 in the global surface oceans and the oceanic Suess effect. *Global Biogeochemical Cycles, 13*, 307–335.

Hannah, C. G., Shore, J. A., Loder, J. W., & Naimie, C. E. (2001). Seasonal circulation on the western and central Scotian Shelf. *Journal of Physical Oceanography*, *31*(2), 591-615.

Hélie, J.-F., Hillaire-Marcel, C., & Rondeau, B. (2001). Seasonal changes in the sources and fluxes of dissolved inorganic carbon through the St. Lawrence River ---- isotopic and chemical constraint. *Chemical Geology*, *186*, 117-138.

Houghton, R.A. (2003). The contemporary carbon cycle. In: Holland, H.D., Turekian, K.K. (Eds.), Treatise on Geochemistry, vol. 8. In: Schlesinger, W. (Ed.), Biogeochemistry. Elsevier, Amsterdam, pp. 473–513.

IPCC (2007). Climate Change 2007: Mitigation. *Contribution of Working Group III to the Fourth Assessment Report of the Intergovernmental Panel on Climate Change* [B. Metz, O.R. Davidson, P.R. Bosch, R. Dave, L.A. Meyer (eds)], Cambridge University Press, Cambridge, United Kingdom and New York, NY, USA.

Keeling, C. D. (1979). The suess effect: ^{13}Carbon-^{14}Carbon interrelations. *Environment International, 2*(4), 229-300.

Le Quéré, C., Moriarty, R., Andrew, R. M., Peters, G. P., Ciais, P., Friedlingstein, P., … Zeng, N., (2014). Global carbon budget 2014. *Earth System Science Data, 7,* 47-85.

Lemay, J., Thomas, H., Craig, S.E., Burt, W.J., Fennel, K., & Greenan, B.J.W. (2018). Hurricane Arthur and its effect on the short-term variability of pCO_2 on the Scotian Shelf, NW Atlantic. *Biogeosciences*, *15*, 2111-2123.

Loder, J.W., Han, G., Hannah, C.G., Greeenberg, D.A., & Smith, P.C. (1997). Hydrography and baroclinic circulation in the Scotian Shelf region: winter versus summer. *Canadian Journal of Fisheries and Aquatic Sciences*. *54*, 40–56.

Lynch-Stieglitz, J., Stocker, T. F., Broecker, W. S., & Fairbanks, R. G. (1995). The influence of air-sea exchange on the isotopic composition of oceanic carbon: observations and modeling. *Global Biogeochemical Cycles*, *9*(4), 653-665.

Mackensen, A. (2013), High epibenthic foraminiferal δ13C in the recent deep Arctic Ocean: implications for ventilation and brine release during stadials, *Paleoceanography, 28*, 574–584. Retrieved from https://doi.org/10.1002/palo.20058

Michaelis, J., Usdowski, E., & Menschel, G. (1985). Partitioning of/sup 13/C and/sup 12/C on the degassing of CO/sub 2/and the precipitation of calcite-Rayleigh-type fractionation and a kinetic model. *Am. J. Sci.;(United States)*, *285*(4).

Montenegro, A., Brovkin, V., Eby, M., Archer, D., & Weaver, A. J. (2007). Long term fate of anthropogenic carbon. *Geophysical Research Letters*, *34*(19).

Mook, W., J. Bommerson, & W. Staverman (1974), Carbon isotope fractionation between dissolved bicarbonate and gaseous carbon dioxide, Earth Planet. Sci. Lett., 22(2), 169–176, doi:10.1016/0012-821X(74)90078-8.

Mucci, A., Starr, M., Gilbert, D., & Sundby, B. (2011). Acidification of Lower St. Lawrence Estuary Bottom Waters, *Atmosphere-Ocean*, *49*(3), 206-218. doi:10.1080/07055900.2011.559265

NASA (2019). Global Climate Change. Carbon dioxide. Retrieved from https://climate.nasa.gov/vital-signs/carbon-dioxide/

Ninnemann, U. S., & Charles, C. D. (1997). Regional differences in Quaternary Subantarctic nutrient cycling: Link to intermediate and deep water ventilation. *Paleoceanography, 12*(4), 560–567

NOAA. (2005). The technical details: chemistry composition of an atom. Retrieved from https://www.esrl.noaa.gov/gmd/ccgg/isotopes/chemistry.html

Olsen, A., & Ninnemann, U. (2010). Large 13C gradients in the preindustrial North Atlantic revealed. *Science, 330*, 658–659.

O'Leary, M. H. (1981). Carbon isotope fractionation in plants. *Phytochemistry*, *20*(4), 553-567.

O'Leary, M. H. (1988). Carbon isotopes in photosynthesis. *Bioscience*, *38*(5), 328-336.

Orr, J. C., Fabry, V. J., Aumont, O., Bopp, L., Doney, S. C., Feely, R. A., …Yool, A. (2005). Anthropogenic ocean acidification over the twenty-first century and its impact on calcifying organisms. *Nature*, *437*, 681–686. doi:10.1038/nature04095

Osterroht, C., & Thomas, H. (2000). New production enhanced by nutrient supply from non-Redfield remineralisation of freshly produced organic material. *Journal of Marine Systems*, *25*(1), 33-46.

Ostle, C., Johnson, M., Landschützer, P., Schuster, U., Hartman, S., Hull, T., & Robinson, C. (2015). Net community production in the North Atlantic Ocean derived from Volunteer Observing Ship data. *Global Biogeochemical Cycles*, *29*(1), 80-95.

Ostrom, N. E., Macko, S. A., Deibel, D., & Thompson, R. J. (1997). Seasonal variation in the stable carbon and nitrogen isotope biogeochemistry of a coastal cold ocean environment. *Geochimica et Cosmochimica Acta*, *61*(14), 2929-2942.

Parry, M., Parry, M. L., Canziani, O., Palutikof, J., Van der Linden, P., & Hanson, C. (Eds.). (2007). *Climate change 2007-impacts, adaptation and vulnerability: Working group II contribution to the fourth assessment report of the IPCC* (Vol. 4). Cambridge University Press.

Parizek, B. R., & Alley, R. B. (2004). Implications of increased Greenland surface melt under global-warming scenarios: ice-sheet simulations. *Quaternary Science Reviews*, *23*(9-10), 1013-1027.

Petrie, B., & Drinkwater, K. (1993). Temperature and salinity variability on the Scotian Shelf and in the Gulf of Maine 1945–1990. *Journal of Geophysical Research: Oceans*, *98*(C11), 20079-20089.

Quay, P. D., Tilbrook, B., & Wong, C. S. (1992). Oceanic uptake of fossil fuel CO2: Carbon-13 evidence, Science, 256, 74–79.

Quay, P., Sonnerup, R., Strutsman, T.W., & McNichol, A. (2003). Changes in the $^{13}C/^{12}C$ of dissolved inorganic carbon in the ocean as a tracer of anthropogenic CO_2 uptake. *Global Biogeochemical Cycles. 17*, 1004-1018.

Quay, P., & Stutsman, J. (2003). Surface layer carbon budget for the subtropical N. Pacific: ^{13}C constraints at station Aloha. *Deep-Sea Research I, 50*, 1045–1061.

Quay, P., R. Sonnerup, J. Stutsman, J. Maurer, A. Körtzinger, X. Padin, & C. Robinson. (2007). Anthropogenic CO_2 accumulation rates in the North Atlantic Ocean from changes in the $^{13}C/^{12}C$ of dissolved inorganic carbon, *Global biogeochemical cycles, 21*.

Rutherford, K., & Fennel, K. (2018). Diagnosing transit times on the northwestern North Atlantic continental shelf. *Ocean Science, 14*, 1207-1221.

Sackett, W. M., & Moore, W. S. (1966). Isotopic variations of dissolved inorganic carbon. *Chemical Geology*, *1*, 323-328.

Sackett, W. M., Eckelmann, W. R., Bnder, M. L., & Bé, A. W. H. (1965). Temperature dependence of carbon isotope composition in marine plankton and sediments. *Science*, *148*(3667), 235-237.

Schmittner, A., Gruber, N., Mix, A. C., Key, R. M., Tagliabue, A., & Westberry, T. K. (2013). Biology and air-sea gas exchange controls on the distribution of carbon isotope ratios (delta C-13) in the ocean. *Biogeosciences*, *10*(9), 5793-5816.

Serret, P., C. Robinson, E. Fern.ndez, E. Teira, G. Tilstone, and V. P.rez (2009), Predicting plankton net community production in the Atlantic Ocean, *Deep Sea Research*, Part II, *56*(15), 941–953, doi:10.1016/j.dsr2.2008.10.006.

Shadwick, E.H. (2010). Carbon cycling in Canadian coastal waters: Process studies of the Scotian Shelf and the Southeastern Beaufort Sea. Halifax, NS. Dalhousie University Press.

Shadwick, E.H., & Thomas, H. (2014). Seasonal and spatial variability in the CO_2 system on the Scotian Shelf (Northwest Atlantic). *Marine Chemistry. 160*, 42-55.

Shadwick, E. H., Thomas, H., Azetsu-Scott, K., Greenan, B. J. W., Head, E., & Horne, E. (2011). Seasonal variability of dissolved inorganic carbon and surface water pCO_2

in the Scotian Shelf region of the Northwestern Atlantic. *Marine Chemistry, 124*(1-4), 23-37.

Shan, S. (2016). Eulerian and Lagrangian Studies of Circulation on the Scotian Shelf and Adjacent Deep Waters of the North Atlantic with Biological Implications.

Smith, S. V., & Hollibaugh, J. T. (1993). Coastal metabolism and the oceanic organic carbon balance. *Reviews of Geophysics*, *31*(1), 75-89.

Smith, P. C., Flagg, C. N., Limeburner, R., Fuentes-Yaco, C., Hannah, C., Beardsley, R. C., & Irish, J. D. (2003). Scotian Shelf crossovers during winter/spring 1999. *Journal of Geophysical Research: Oceans*, *108*(C11).

Solomon, S., Plattner, G. K., Knutti, R., & Friedlingstein, P. (2009). Irreversible climate change due to carbon dioxide emissions. *Proceedings of the national academy of sciences*, *106*(6), 1704-1709.

Spiker, E. (1980). The behavior of C-14 and C-13 in estuarine water; effects of in situ CO_2 production and atmospheric change, *Radiocarbon, 22*, 647–654.

Takahashi, T., Olafsson, J., Goddard, J., Chipman, D.W., & Sutherland, S.C., (1993). Seasonal variation of CO2 and nutrients in the high-latitude surface oceans: a comparative study. *Global Biogeochemical Cycles, 7*, 843-878.

Tans, P. P. (1980), On calculating the transfer of carbon-13 in reservoir models of the carbon cycle, Tellus, 32, 464–469.

Thomas, H., Bozec, Y., de Baar, H. J., Borges, A., & Schiettecatte, L. S. (2005). Controls of the surface water partial pressure of CO2 in the North Sea. *Biogeosciences*, *2*(4), 323-334.

Thomas, H., Schiettecatte, L. S., Suykens, K., Koné, Y.J.M., Shadwick, E.H., Prowe, A.E.F., Bozec, Y., … Borges, A.V. (2009). Enhanced ocean carbon storage from anaerobic alkalinity generation in coastal sediments. *Biogeosciences*, 6, 267-274.

Thomas, H., & Schneider, B. (1999). The seasonal cycle of carbon dioxide in Baltic Sea surface waters. *Journal of Marine Systems*, *22*(1), 53-67.

Thomas, H., Craig, S. E., Greenan, B. J. W., Burt, W., Herndl, G. J., Higginson, S., ... & Urrego-Blanco, J. (2012). Direct observations of diel biological CO 2 fixation on the Scotian Shelf, northwestern Atlantic Ocean. *Biogeosciences*, *9*(6), 2301-2309.

Townsend, D. W., Pettigrew, N. R., Thomas, M. A., Neary, M. G., McGillicuddy, J., Dennis, J., & O'Donnell, J. (2015). Water masses and nutrient sources to the Gulf of Maine. *Journal of Marine Research*, *73*(3-4), 93-122.

Umoh, J. U., & Thompson, K.R. (1994). Surface heat flux, horizontal advection, and the seasonal evolution of water temperature on the Scotian Shelf. *Journal of Geophysical Research. 99* (20), 403-416.

Urrego-Blanco, J., & Sheng, J. (2012). Interannual variability of the circulation over the eastern Canadian shelf. *Atmosphere-Ocean*, *50*(3), 277-300.

Vandemark, D., Salisbury, J. E., Hunt, C. W., Shellito, S. M., Irish, J. D., McGillis, W. R., ... & Maenner, S. M. (2011). Temporal and spatial dynamics of CO2 air-sea flux in the Gulf of Maine. *Journal of Geophysical Research: Oceans*, *116*(C1).

Weare, B. C., & Newell, R. E. (1977). Empirical orthogonal analysis of Atlantic Ocean surface temperatures. *Quarterly Journal of the Royal Meteorological Society*, *103*(437), 467-478.

Winde, V., Böttcher, M. E., Escher, P., Böning, P., Beck, M., Liebezeit, G., & Schneider, B. (2014a). Tidal and spatial variations of δ and aquatic chemistry in a temperate tidal basin during winter time. *Journal of Marine Sciences, 129*, 396- 404.

Winde, V., M. E. Böttcher, P. Escher, P. B€oning, M. Beck, G. Liebezeit, & B. Schneider. (2014b). Corrigendum to: Tidal and spatial variations of DI13C and aquatic chemistry in a temperate tidal basin during winter time. [J. Mar. Sys. 129: 396–404]. *Journal of Marine Sciences*, *139*, 509. doi:10.1016/j.jmarsys.2014.09.008

Wollast, R. (1998). Evaluation and comparison of the global carbon cycle in the coastal zone and in the open ocean. *The sea*, *10*, 213-252.

Wong, W. W., & Sackett, W. M. (1978). Fractionation of stable carbon isotopes by marine phytoplankton. *Geochimica et Cosmochimica Acta*, *42*(12), 1809-1815.

Zeebe, R. E., & Wolf-Gladrow, D. (2001). *CO_2 in seawater: equilibrium, kinetics, isotopes* (No. 65). Gulf Professional Publishing.

Zhang, J., & Quay, P. D. (1997). The total organic carbon export rate based on13C and12C of DIC budgets in the equatorial Pacific region. *Deep Sea Research Part II: Topical Studies in Oceanography*, *44*(9-10), 2163-2190.